A SIMULATION TOOL FOR STUDYING THE EFFECTS OF SPECIAL PROTECTION SYSTEMS AND COMMUNICATIONS ON POWER SYSTEM STABILITY

By

SANJOY KUMAR SARAWGI

A thesis submitted in partial fulfillment of
the requirements for the degree of

MASTER OF SCIENCE IN ELECTRICAL ENGINEERING

WASHINGTON STATE UNIVERSITY
School of Electrical Engineering and Computer Science

AUGUST 2004

To the Faculty of Washington State University:

The members of the Committee appointed to examine the thesis of SANJOY KUMAR SARAWGI find it satisfactory and recommend that it be accepted.

Chair

ACKNOWLEDGEMENT

I would like to express my deepest gratitude to my academic and research advisor Dr. Anjan Bose for his guidance and constant support in helping me to conduct and complete this work. He has been a great source of inspiration. I also want to thank Dr. Kevin Tomsovic and Dr. V. Mani Venkatasubramanian for serving on my advisory committee, as well as for their generous advice from time to time during the course of this work.

Many thanks to all the people I have come to know in Washington State and Pullman, whose friendship and companionship I will always enjoy. I owe my sincere appreciation to my family and relatives who have been a constant support and encouragement. Finally, I want to extend my profound appreciation to my brother for his love, affection, invaluable support and sacrifice during my life and studies.

This work was partially supported by the Consortium of Electric Reliability Technology Solutions (CERTS) and the Power Systems Engineering Research Center (PSERC).

CERTS is funded by the Assistant Secretary of Energy Efficiency and Renewable Energy, Office of the Distributed Energy and Electric Reliability, Transmission Reliability Program of the U. S. Department of Energy.

PSERC is a National Science Foundation Industry University Cooperative Research Center (NSF IUCRC) funded by NSF and a consortium of about 40 companies in the power industry.

I sincerely acknowledge the financial support extended to this project by the sponsors.

A SIMULATION TOOL FOR STUDYING THE EFFECTS OF SPECIAL PROTECTION SYSTEMS AND COMMUNICATIONS ON POWER SYSTEM STABILITY

Abstract

by Sanjoy Kumar Sarawgi, MS
Washington State University
August 2004

Chair: Anjan Bose

Wide-area real-time measurement equipment, particularly phasor measurement technology, and associated communication networks make the application of advanced control techniques potentially promising. The use of wide-area measurements and broadband optical communication networks for real-time feedback control may finally be a reality. The overall goal of this research work was to develop a simulation tool to investigate the potential application of wide-area measurement, protection and control actions to improve the real-time response of power systems to otherwise damaging disturbances. Effects of communication system delay/failure on the system dynamic response can also been investigated using this tool. Dynamic responses were observed for some select cases of instability, on the IEEE 39-bus system using this tool. Wide-area control actions were then determined to stabilize the system. This simulation tool can be used for voluminous offline studies to determine such wide-area control actions for power system. Modeling the communication system in this simulation program makes it particularly attractive because the effect of communication delay/failure on dynamic response can be studied together with power system dynamics.

Keywords: Power System Modeling, System Dynamics, Transient Stability, Protective Relays, Special Protection Scheme (SPS), Communication, WACS.

Dedicated to My Brother, Sandip

Contents

List of Figures

List of Tables

Chapter 1

Introduction

During the last decades, power systems around the world have suffered a number of severe disturbances, breakdowns and voltage collapses [1, 2, 3, 4]. These problems are mostly related to high levels of stress in the networks. Because of environmental and political considerations, it is hard to obtain permission to build new transmission lines in many industrialized countries. These restrictions along with the fact that utilities face continuous growth of power demand and power market deregulation, power systems are operated closer to their stability limits. Hence, the existing networks must transmit more power, making them more vulnerable at the same time. In such a scenario, a disturbance, such as a line or power plant outage, may initiate instability and could lead to a system collapse.

1.1 Background and Motivation

Instability phenomena in power systems can be classified and defined as follows [5]:

- **Frequency Instability** – is the inability of a power system to maintain steady frequency within the operating limits.
- **Voltage Instability** – is the inability of a power system to maintain steady

acceptable voltages at all buses in the system under normal operating conditions and after being subjected to a disturbance. A system enters a state of voltage instability when a disturbance, increase in load demand, or change in system conditions causes an uncontrollable drop in voltage. According to Kundur, "A system is voltage unstable if, for at least one bus in the system, the bus voltage magnitude decreases as the reactive power injection in the same bus is increased".

- **Transient Angular Instability** (also called Generator's Out-of-step) – is the state of the power system when it is unable to maintain synchronism when subjected to a severe transient disturbance. The resulting system response involves large excursions of generator angles and is influenced by the nonlinear power-angle relationship.

- **Local mode of Small-signal Angular Instability** (also mentioned as Generator's Swinging or Power Oscillations) – is the inability of the power system to maintain synchronism under small disturbances. Such disturbances occur continually on the system because of small variations in loads and generation. The disturbances are considered sufficiently small for linearization of system equations to be permissible for purposes of analysis. *Local modes* or *machine-system modes* are associated with the swinging of units at a generating station with respect to the rest of the power system.

The interruption in power delivery that follows a system collapse has economic consequences such as loss of income for the power utility and lost production for affected industries. Great efforts are being made to determine the correct protective action for impending system instability. With sufficient knowledge, correct emergency actions can be taken in case of such instability scenarios to stabilize the system, thus preventing cascade trippings and blackouts.

In the beginning, attempts to apply local protection devices were made. However the character of the dangerous stresses mentioned above, is often global, not local. Therefore the protection systems, using data from more locations as well as acting with a wide-area orientation, have been proposed, designed and in some cases installed to handle them [6]. These are most often referred to as Special Protection Schemes (SPS) or System Protection Schemes.

According to Anderson, *et* al., they are defined as: ***"... a protection scheme that is designed to detect a particular system condition that is known to cause unusual stress to the power system and to take some type of predetermined action to counteract the observed condition in a controlled manner. In some cases, SPSs are designed to detect a system condition that is known to cause instability, overload, or voltage collapse. The action prescribed may require the opening of one or more lines, tripping of generators, ramping of HVDC power transfers, intentional shedding of load, or other measures that will alleviate the problem of concern. Common types of line or apparatus protection are not included in the scope of interest here"*** [7].

Design of any system is followed by extensive testing, before it can be actually implemented. But it is not possible to carry out tests on a real power system because of the risks involved. Many studies are therefore made using a simulation approach. Detailed models of system components have been developed and are used in computer programs for dynamic simulations. One problem with these programs is that they are designed to work under certain conditions. If these conditions are not fulfilled, which can be the case in stability studies, the programs might give a wrong solution or no solution at all. Hence, careful consideration should be given to the choice of these models so that they represent the system phenomena as closely as possible to the required accuracy.

1.2 General Overview of the Problem

The increasing popularity of wide-area measurement and controls in power systems today, calls for more powerful software tools, having models for protective relay and capability to simulate the effects of communication system and wide-area control schemes on system dynamics. Power system dynamic simulation programs, currently available, although very powerful, do lack in some or all of the above mentioned requirements. Though almost all of them can handle system disturbances like line or generator or load outages, these disturbances have to be defined before the program is actually executed. Protective relay modeling in such cases becomes a very difficult task using these programs. However, the importance of relay modeling cannot be better emphasized than by citing the conclusion of the Swedish blackout [8], which said "normal stability methods were insufficient to explain the system behavior that led to cascade tripping." According to Perez *et* al., this was because "among other factors, relay protection was not modeled in the dynamic analysis" [9]. Though some programs (e.g. ETMSP, STAG[10] and GE-PSLF) have the capability to model relays, representation of a communication network to study the effects of communication delay on system stability is very involved. It requires additional programming to simulate the effects of a communication network and is not very flexible. Thus the need for a new integrated simulation tool was felt, which can simulate the system dynamic response along with the protective relays and communication system.

The primary objective of this work was developing a simulation tool for system dynamic studies which integrate the protection, communication and wide area measurement and control system in the dynamic simulation program, so that it can simulate relay logic and actions and data communication effects. Automatic breaker and recloser actions are included in the simulation. For a given communication configuration, delays in measurement data and control signals are predetermined and

are incorporated into the program as fixed time-delays before the action due to that signal/measurement is taken. The program is then used for stability studies on the IEEE 39-Bus system. Since the system base case is stable it is stressed to get cases of instability. This is accomplished by increasing generation in one part of the system and an equivalent amount of load in some other part, such that the power flows through key lines connecting these two parts of the system are high. *Special Protection Schemes,* were determined for two different cases of instability and implemented in the program. Studies were performed to observe the effects of communication delay/failure, using this schemes, on system dynamic response and stability.

1.3 Research Goals and Approach

This work has a two-fold objective. The main intention is to provide a novel simulation tool for system dynamic study of a power system, where effects of protective relay actions and communication network delays on system stability can be studied. To this effect, programs in MATLAB have been written which simulate the dynamics of electric power systems in the time domain. Besides the models for synchronous machines, loads, exciters, governors and power system stabilizers; protective relays have also been modeled. Effects of such local relay protection system have been included as an integral part of the program. Thus, cascading events can be observed. Simulation of communication effects has been accomplished by introducing predetermined time delays before relay/control actions are taken.

The work also includes case studies on a test system where different instability phenomena, such as *transient angular instability and local mode of small-signal angular instability* could be observed. Such cases were obtained by modifying the generations and loads in the system to make it more stressed. This is justified by the fact that power systems today are facing severe transmission stresses due to

increasing loads with little or no transmission capacity being added. These instabilities could not be countered by the local relay protection system. Hence, special attention has been focused on determining special protection schemes. Different wide-area controls were tried, and suitable schemes for particular test cases of instability were determined. Such wide-area Special Protection Schemes were simulated in the program together with their communications systems.

1.4 Outline of the Thesis

This thesis work is divided into six chapters. In Chapter 1, an introduction to the stability problem in the modern-day power system is presented with special emphasis on transient stability. The importance of Wide-Area Control Systems (WACS) and Special Protection Schemes has been stressed. Next, the role of computer simulation of power system is discussed. Sec. 1.3 lists the research goals and briefly explains the adopted approach.

In Chapter 2, models used for the system components are described. the differential-algebraic equations describing the dynamics of the system are presented here. Descriptions of the relay and communication systems and the special protection schemes implemented are provided in Chapter 3.

Chapter 4 presents the simulation approach. It describes the programs and algorithms used in the simulation. Implementation of the protection, communication and special protection schemes are also explained here.

Once the simulation program was developed it was tested on the IEEE 39 Bus systems. Results obtained for dynamic stability studies on the test system are presented in Chapter 5.

Finally, conclusions and the scope of future work on this topic are mentioned in Chapter 6.

The IEEE 39-Bus system has been used as the test system for this work. Ap-

pendix A contains the power flow and dynamic data for this system. A single line diagram is also included.

Chapter 2

System Component Modeling

2.1 The System Dynamic Model

The dynamic models for the simulation of the power system dynamics, presented here, includes field flux decay generator model, Automatic Voltage Regulator (AVR), Speed Governor Control through a governor and Power System Stabilizer (PSS). This program employs a fourth order (two-axis) model of a generator. For exciter modeling, an IEEE Type-I DC exciter is used. A simple governor model and PSS have also been included in the program. Loads have been modeled using the ZIP model where the load composition can be user-defined. The various models are described in the following sections.

2.1.1 Synchronous Generator Model

Synchronous generators form the principal source of electric energy in power systems. Many large loads are driven by synchronous motors. Synchronous condensers are sometimes used as means of providing reactive power compensation and controlling voltage. These devices operate on the same principle and are collectively referred to as synchronous machines. The power system stability problem is largely

one of keeping interconnected synchronous machines in synchronism. Therefore an accurate modeling of their dynamic performance is of fundamental importance to the study of power system stability.

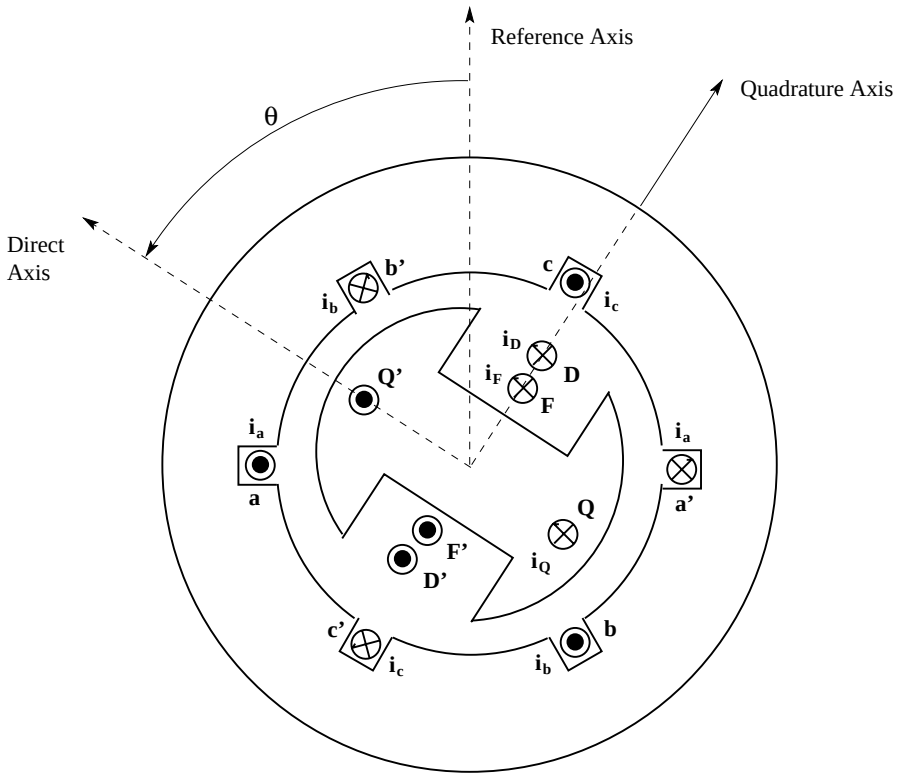

Figure 2.1: Synchronous generator schematic diagram

There exists a rich history on the modeling of synchronous generators and the dynamic models can vary a great deal in terms of their complexity [5]. In this work, a fourth-order (two axis) model, as described in [11], has been used.

The dynamic equations of the synchronous generator for the two-axis model can be stated as [5, 11]:

$$\dot{\delta} = (\omega - 1)\,\omega_s \tag{2.1}$$

$$2H\dot{\omega} = P_m - P_g - K_D\,(\omega - 1) \tag{2.2}$$

$$T_{d0}^{'}\dot{E}_q^{'} = -E_q^{'} - \left(x_d - x_d^{'}\right) I_d + E_{fd} \tag{2.3}$$

$$T_{q0}^{'}\dot{E}_d^{'} = -E_d^{'} - \left(x_q - x_q^{'}\right) I_q \tag{2.4}$$

Here, the four state variables are: δ, the rotor angle, ω, the rotor frequency in per unit, $E_q^{'}$ the internal quadrature-axis voltage and $E_d^{'}$, the internal direct-axis voltage. H is the inertia constant of the generator, P_m and P_g are the input mechanical power and the output electrical power of the generator and K_D the damping coefficient. $T_{d0}^{'}$ and $T_{q0}^{'}$ are the direct and quadrature axis transient field winding time constants and x_d, $x_d^{'}$, x_q and $x_q^{'}$ are the corresponding synchronous and transient reactances.

The equations relating the external bus quantities and the internal machine transformed (Park's) quantities are:

$$V_d = V sin\,(\delta - \theta) \tag{2.5}$$

$$V_q = V cos\,(\delta - \theta) \tag{2.6}$$

$$P_g = V_d I_d + V_q I_q \tag{2.7}$$

$$Q_g = V_d I_q - V_q I_d \tag{2.8}$$

$$V^2 = V_d^2 + V_q^2 \tag{2.9}$$

$$I_g^2 = I_d^2 + I_q^2 \tag{2.10}$$

The external bus voltage has magnitude V and phase θ. P_g and Q_g are the generator internal real and reactive power injections. The variables V_d and V_q are the components of the bus voltage after they are transformed into the internal Park coordinate frame that is rotating synchronously with the rotor. The effect of Park's transformation is simply to transform all stator quantities from phases a, b and c

into new variables, the frame of reference of which moves with the rotor. This leads to great simplification in the mathematical description of the synchronous machine. The transformation depends on the difference in phase $\delta - \theta$, between the terminal voltage and the internal rotor angle. Similarly, I_d and I_q are the Park transformed components of the terminal current I_g.

2.1.2 Exciter Model

In this study the standard IEEE type DC1A exciter model was used. This model, described by the block diagram of Fig. 2.2, is used to represent field controlled dc commutator exciters with continuously acting voltage regulators (especially the direct-acting rheostatic, rotating amplifier, and magnetic amplifier types). The exciter may be separately excited or self excited, the latter type being more common. When self excited (the voltage regulator operating in *buck-boost* mode), K_E is selected so that initially $V_A = 0$ [5], representing operator action of tracking the voltage regulator by periodically trimming the shunt field rheostat set point. A value of $K_E = 1$ is used to represent a separately excited exciter. The major time constant, T_A, and gain, K_A, associated with the voltage regulator are shown incorporating non-windup limits typical of saturation or amplifier power supply limitations.

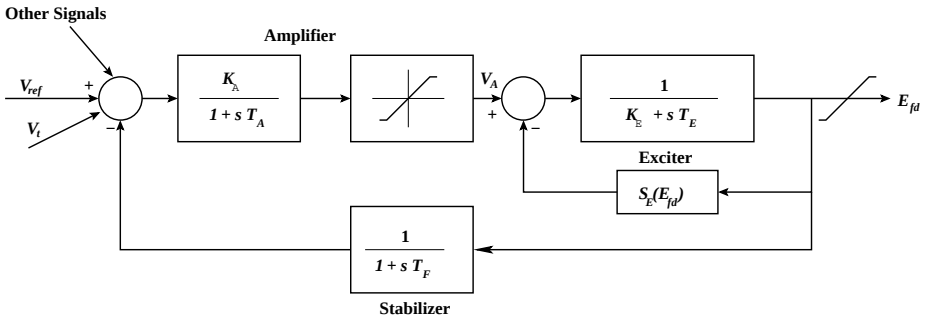

Figure 2.2: IEEE DC1A exciter block diagram

The mathematical model representing the dynamics of this exciter is given by

the following equations:

$$T_A\dot{V_A} = -V_A + K_A(V_{ref} - V - V_F - V_S) \quad (2.11)$$

$$T_E\dot{E_{fd}} = -K_E E_{fd} + V_A - S_{ex}(E_{fd})E_{fd} \quad (2.12)$$

$$T_F\dot{V_F} = -V_F + K_F\dot{E_{fd}} \quad (2.13)$$

The term $S_{ex}(E_{fd})$ is a nonlinear function with a value defined at any chosen E_{fd}. The output of this saturation block, is the product of the input, E_{fd}, and the value of the nonlinear function, $S_{ex}(E_{fd})$, at this exciter voltage. V_S is a supplementary stabilizing signal from the PSS.

2.1.3 Governor Model

The prime mover provides the mechanism for controlling the synchronous machine speed and hence voltage frequency. In order to automatically control speed (and therefore frequency), a device must sense either speed or frequency in such a way that comparison with a desired value can be used to create an error signal to take corrective action. The block diagram of such a basic model for a time constant governor with speed regulation R is shown in Fig. 2.3:

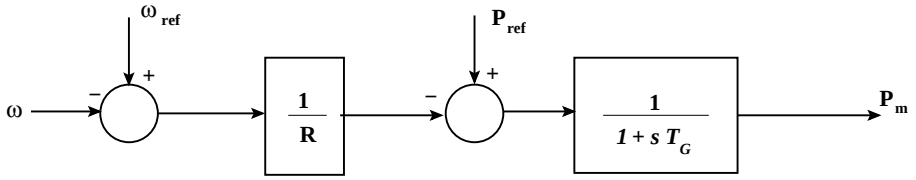

Figure 2.3: Governor model block diagram

The governor block can be mathematically represented as:

$$T_G\dot{P_m} = -P_m + P_{ref} - \frac{1}{R}(\omega - 1) \quad (2.14)$$

2.1.4 Power System Stabilizer (PSS) Model

A PSS can be viewed as an additional control block used to enhance the system stability. This block is added to the AVR, and uses stabilizing feedback signals such as shaft speed, terminal frequency and/or power to change the input signal of the AVR. Power system dynamic performance is improved by the damping of system oscillations.

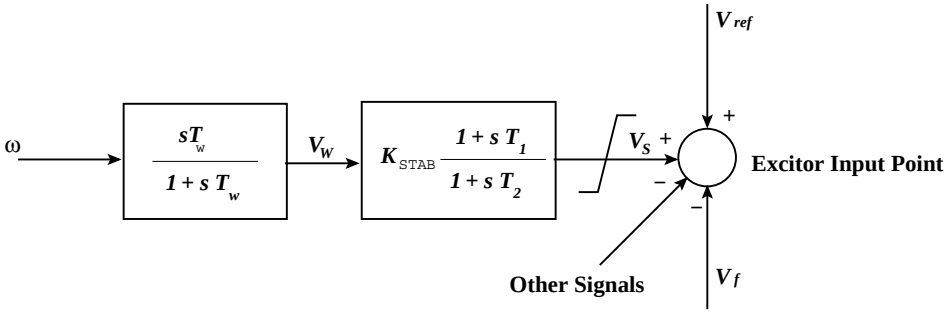

Figure 2.4: Block Diagram of a simple PSS model

The basic blocks of a typical PSS model, are illustrated in Fig. 2.4. The first is the washout block, which serves as a high-pass filter, with a time constant that allows the signal associated with oscillations in rotor speed to pass unchanged, but does not allow the steady state changes to modify the terminal voltages. The other one is the phase compensation block, which provides the desired phase-lead characteristic to compensate for the phase lag between the AVR input and the generator electrical (air-gap) torque; in practice, two or more first-order blocks may be used to achieve the desired phase compensation. The stabilizer gain, K_{STAB}, which determines the amount of damping can be represented by a separate block before the washout block or it can be coupled with the phase compensator as shown above. The differential equations describing a single- stage PSS as shown in Fig. 2.4 are:

$$T_W \dot{V_W} = -V_W + T_W \dot{\omega} \tag{2.15}$$

$$T_2 \dot{V_S} = -V_S + K_{STAB} V_W + K_{STAB} T_1 \dot{V_W} \tag{2.16}$$

Besides the component dynamic models given above, the models used in the program for loads and transformers are described in the following sections.

2.2 Load Model

The modeling of loads in stability studies is a complex problem due to the unclear nature of aggregated loads (e.g. a mix of fluorescent, compact fluorescent, incandescent lamps, refrigerators, heater, motor, etc.). Load models are typically classified into two broad categories: static and dynamic. The loads can be modeled using constant impedance, constant current and constant power static load models. Thus,

1. *Constant Impedance Load Model (constant Z)*: A static load model where the real and reactive power is proportional to the square of the voltage magnitude. It is also referred to as constant admittance load model.

2. *Constant Current Load Model (constant I)*: A static load model where the real and reactive power is directly proportional to the voltage magnitude.

3. *Constant Power Load Model (constant P)*: A static load model where the real and reactive powers have no relation to the voltage magnitude. It is also referred to as constant MVA load model.

These load models, can be described by the following polynomial equations [12]:

$$P_L = kP_0\left[A_1 + A_2\frac{V}{V_0} + A_3\left(\frac{V}{V_0}\right)^2\right] \tag{2.17}$$

$$Q_L = kQ_0\left[B_1 + B_2\frac{V}{V_0} + B_3\left(\frac{V}{V_0}\right)^2\right] \tag{2.18}$$

where, $A_1 + A_2 + A_3 = B_1 + B_2 + B_3 = 1$; P_0 and Q_0, the so-called nominal powers, are the load real and reactive powers consumed under nominal conditions i.e., at the reference voltage V_0 and the nominal frequency f_0. The actual or consumed load

powers P_L and Q_L are the powers consumed by the load under existing conditions of voltage V and frequency f. Although the actual load in a system is usually frequency dependent, this frequency dependence is ignored in this work for simplicity. The value k is an independent demand variable called loading factor. Such a load model is often referred to as the ZIP Load Model.

2.3 Transformer Model

Tap-changing transformers are represented using an equivalent π model shown in Fig. 2.5.

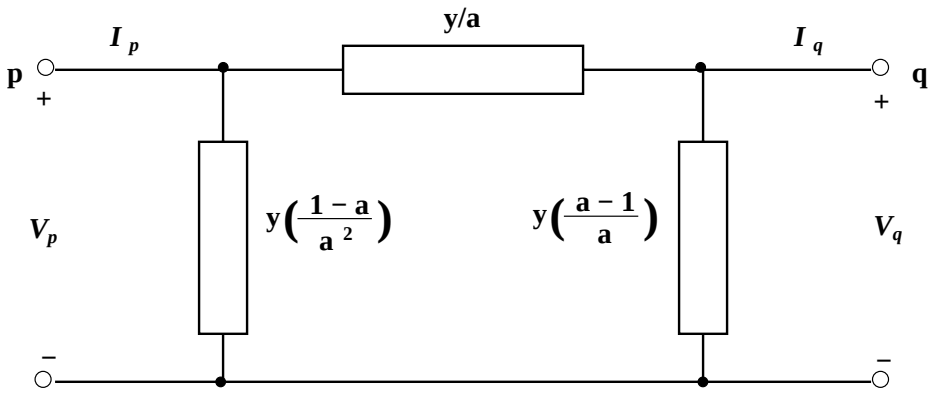

Figure 2.5: Transformer equivalent π model

The equivalent shunt and series admittances for the transformers in the network, obtained using this model, are directly included in the Y-bus.

2.4 The Differential-Algebraic Equations of the System

The synchronous machine model along with the associated regulating devices thus becomes a tenth-order model (ten state variables for each synchronous machine). The dynamic states for this model are:

$$\mathbf{x} = [\omega \ \delta \ E_d^{'} \ E_q{}' \ V_A \ V_F \ E_{fd} \ V_W \ V_S \ P_m]^T$$

Thus, for the i^{th} machine, the 10 differential equations describing its dynamics are:

$$\dot{\delta}_i = (\omega_i - 1)\,\omega_s \tag{2.19}$$

$$2H_i\dot{\omega}_i = P_{mi} - P_{gi} - K_{Di}\,(\omega_i - 1) \tag{2.20}$$

$$T^{'}_{d0i}\dot{E}^{'}_{qi} = -E^{'}_{qi} - \left(X_{di} - X^{'}_{di}\right) I_{di} + E_{fdi} \tag{2.21}$$

$$T^{'}_{q0i}\dot{E}^{'}_{di} = -E^{'}_{di} - \left(X_{qi} - X^{'}_{qi}\right) I_{qi} \tag{2.22}$$

$$T_{Ai}\dot{V}_{Ai} = -V_{Ai} + K_{Ai}(V_{(ref)i} - V_i - V_{Fi}) \tag{2.23}$$

$$T_{Ei}\dot{E}_{fdi} = -K_{Ei}E_{fdi} + V_{Ai} - S_{ex}(E_{fdi})E_{fdi} \tag{2.24}$$

$$T_{Fi}\dot{V}_{Fi} = -V_{Fi} + K_{Fi}\dot{E}_{fdi} \tag{2.25}$$

$$T_{Wi}\dot{V}_{Wi} = -V_{Wi} + T_{Wi}\dot{\omega}_i \tag{2.26}$$

$$T_{2i}\dot{V}_{Si} = -V_{Si} + K_{Si}V_{Wi} + K_{Si}T_{1i}\dot{V}_{Wi} \tag{2.27}$$

$$T_{Gi}\dot{P}_{mi} = -P_{mi} + P_{(ref)i} - \frac{1}{R_i}(\omega_i - 1) \tag{2.28}$$

In the above set of equations the quantities $P_{gi},\ I_{di},\ I_{qi}$ and V_i are still unknown. These quantities can be derived using the following relationship:

$$\begin{bmatrix} I_q \\ I_d \end{bmatrix} = \begin{bmatrix} R_a & X^{'}_d \\ -X^{'}_q & R_a \end{bmatrix}^{-1} \begin{bmatrix} E^{'}_q - V_q \\ E^{'}_d - V_d \end{bmatrix} \tag{2.29}$$

and Eqns. (2.5 - 2.10). We are only left with determining a relationship between $V,\ \theta,\ P_g$ and Q_g which is given by the power flow equations of the system.

For a multimachine system with n_g generators, there are $10n_g$ differential equations. In a stability study dealing with the electromechanical behavior of the power system, the electrical transients in the network involving the inductances and capacitances are neglected, and the network is assumed to be in quasi-steady state. As a result, the network is represented by a system of algebraic equations that governs the relationship between the injected complex powers at the generator buses and the complex voltages at all the other buses based on the fundamental principles of power flow analysis. Since at each instant in time during the transient, the complex power

injected into the network by the synchronous generators varies, a new solution of voltages at all the other buses has to be determined.

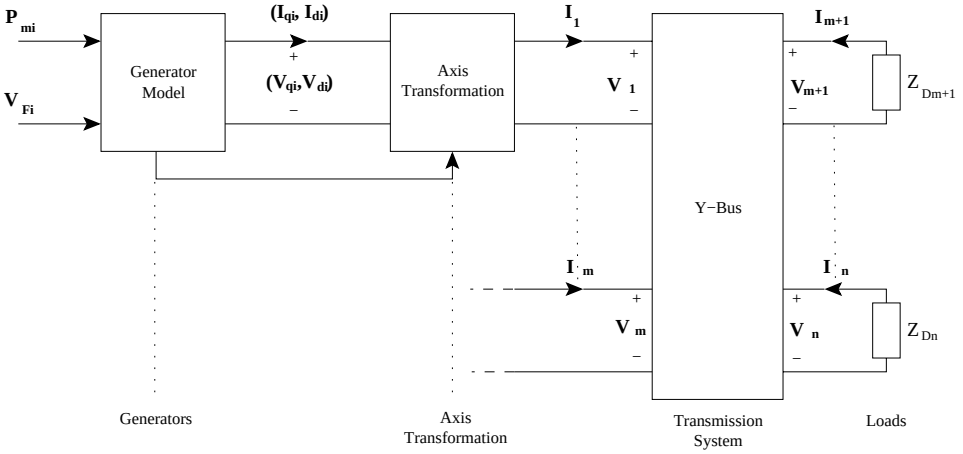

Figure 2.6: An m-machine interconnected Power System

Thus the dynamic simulation program requires the solution of a set of coupled differential-algebraic equations (DAE). The differential equations are the dynamic equation for the generators and the algebraic equation are the power flow equations. These are solved numerically to obtain the condition of the system at each instant in time.

Chapter 3

Relay and Communication Model and Special Protection Schemes

In an actual power system, the system operator has very little interaction with the protection system [13]. The operator is simply an observer of the effects of a disturbance and the resultant relay action. However, this simulation tool provides for specifying a disturbance on command. Thus, the system response will be dictated by the system equations and the resulting operation of the power system relays must be simulated in a realistic way.

3.1 Protective Relay Model

Relay logic usually calls for some limit checking and setting timers. For limit checking the existence of relays will flag certain variables that will have to be limit checked every time those variables are recalculated. There may be more than one limit for a variable, usually a lower and upper limit. When a limit is violated a timer is

initialized. The time-out depends on which limit is violated and in some cases how severe the violation is. At the specified time, circuit breaker statuses are changed as a consequence of the relay operation. Topology changes are then introduced into the simulation as a result of breaker action. If the variable value drops back to an acceptable level before the circuit breaker operation, the timer will reset and the impending circuit breaker action is cancelled.

The following relay models were implemented in this program:

1. *Overfrequency Relay,*
2. *Underfrequency Relay,*
3. *Inverse-time Overcurrent Relay and*
4. *Distance Relays (Zone I and Zone II).*

3.1.1 Overfrequency Relay

Overfrequency due to excess of generation is usually taken care of by the speed governing system on the generator [14]. But the governor action is usually very slow due to its large time constant. Persistent post-fault overfrequency calls for fast overfrequency relays to isolate such generators from the system to protect the generator from damage. Thus, these relays are located on the generator units and they monitor the generator-bus frequency. If the frequency goes beyond a preset value the corresponding generator is tripped and isolated from the system. In this program this value is taken to be 1.025 pu (61.5 Hz). An equivalent amount of load, close to the tripped generator, is also tripped. The amount and location of this load is pre-determined for the system. A fixed time-delay is assumed for this tripping action to take place, to account for breaker action time. Thus, once an overfrequency condition is detected in the program the generator is tripped after

the time delay. It is to be noted here, that the delay is very small since there is no wide-area communication involved in a local relay protection scheme.

3.1.2 Underfrequency Relay

Underfrequency on a generator, or a group of generators, arises from an excess of power demand at the loads compared to the power generated at the generating units. As is the case with overfrequency, the governors are expected to take care of this mismatch in the long run by increasing the generation to match the load. But a severe underfrequency condition requires immediate action which is provided by the underfrequency relays. The obvious relay action would be to drop loads so that the falling frequency can be immediately checked. In this program, the underfrequency relays are set such that if frequency at a generator bus goes below 0.985 pu (59.1 Hz) loads are tripped. Several load shedding schemes have been proposed by [5, 14, 15, 16]. The load shedding scheme is system specific. It depends on the system topology and locations of loads and generations in the system.

3.1.3 Overcurrent Relay

These relays are located mainly on distribution and subtransmission lines and are directional in nature. The time-out setting on the relays is modeled as a simple inverse function of the overcurrent. At the end of each simulation time step, the current flows on the lines are checked against the corresponding thermal overcurrent limits of the lines. There is a timer associated with each relay. If the calculated current $I(t)$ violates the overcurrent limit, *i*.e.,

$$I(t) > I_{lim} \tag{3.1}$$

the timer is set according to,

$$\tau = \frac{1}{I(t)/I_{lim}} \tag{3.2}$$

If the overcurrent sustains for this time duration, the line is tripped. Otherwise the timer is reset and no breaker action is taken. It is important to mention here that the thermal overcurrent limits are dependent on the type of conductors used and the ambient conditions in which they are placed. There is even seasonal variation in these limits [17, 18].

3.1.4 Distance Relays

There are some problems with coordinating time-delay overcurrent relays. The *pickup current* for such relays depend on the maximum load current and minimum fault current and should be between the two [15]. But, the maximum load current depends on the system load and generation, and may increase as the system is stressed more and more. This problem with time-overcurrent relays can be overcome by distance relays, which are more commonly used for high-voltage transmission lines.

A distance relay operates on the basis of a voltage-to-current ratio and is also called a *ratio* or *impedance relay.* Impedance relays are used whenever overcurrent relays do not provide adequate protection. They function even if the short circuit current is relatively low. The speed of operation is independent of current magnitude.

In general, distance protection includes three zones of protection, with each zone reaching a fixed preset distance and operating after a preset time delay from the fault detection instant.

Zone 1 reaches 80–90 % of the protected line. The tripping is instantaneous. Thus for 80% protection, if the voltage-current ratio measured at a bus is less than 80% of the line impedance the relay coil picks up and the breaker is opened instantaneously.

Zone 2 extends beyond the protected line up to about 50% of the adjacent line.

The tripping has a time delay, usually set to a value between 0.3 s to 0.5 s.

Zone 3 covers the entire protected line and the adjacent line. The tripping delay is between 0.6 s to 1.0 s.

In this program only Zone–1 and Zone–2 distance relays with directional feature have been implemented. The Zone–1 relay provides primary protection for 90% of the line. The Zone–2 protection extends up to 25% of the adjacent line.

3.2 Communication System Model

Communication systems are crucial in a wide-area measurement and control system. These systems distribute and manage the information, which is then used for analysis and control/protection of the system. Typical features of present day wide-area measurement and control systems include synchronized positive sequence phasor measurements, digital fiber optics communications from the high-voltage substations, a real-time control computer and output communications for control actions.

To meet the reliability and security requirements, the communication network needs to be designed for fast, robust and reliable operation. A number of factors contribute to achieve these objectives: type and topology of the communication network, communication protocols and media used are among the most important. The speed of the communication system is a function of the communication protocol and the media bandwidth, the frequency and volume of information communicated and the handling of communication errors.

Presently, electrical utilities use a combination of analog and digital communication systems for their operations consisting of: power line carriers, radio channels including microwaves, leased/switched/dedicated phone lines and optical multiplexers. Provided that the type and volume of information that needs to be transferred is adequate, any of these systems will perform well in a wide-area protection and

control system.

Optical systems offer the best performance as a communication medium to an electrical utility. That is due to its immunity to electromagnetic interference and signal fading, and its extremely large bandwidth, which allows for transfer of large quantities of data in real-time. In large scale applications, data transfer latency times of the order of 1-10 ms between any two points in the system is typical [12].

For first swing transient stability, control action must be taken prior to the peak of the forward interarea swing – the sooner the better. Undamped dynamic systems have low oscillation frequency allowing more time for control actions. But, for first swing instability, control action is needed within a few cycles. A discussion on the communication system delays installed for power system is given in [19]. The typical delay time for phasor measurement, fiber optic communications, phasor data concentrator throughput, transfer trip and circuit breaker tripping/closing are approximately 3,2,2,1 and 2/5 60 Hz cycles or around 10 cycles for tripping and 13 cycles for closing (167 and 217 ms). Intentional time delay and throughput delay will be 67 ms or longer.

For this work two different communication topologies were simulated. The *mesh topology* assumes the communication network similar to the power transmission network with communication nodes at the substations and communication links along the power lines. The entire system is divided into three areas with no inter-area communication links. Each of these areas has a data concentrator, which is located at a specified node in the area. Data is routed from the nodes to the data concentrator through the communication links. Since data from different nodes takes different paths and the number of hops in each case might differ, the data concentrator needs to synchronize and time stamp the data before passing it to the control center above it. The control center processes this data to decide if some control actions are required and generates those control signals. The control signal/s from the control

center is likewise routed down to the nodes (substations) where the control device is located. For the purpose of this work, the communication routes are assumed to be the one which lead to a minimum number of hops from the substation (bus) to the control center. However other links leading to alternate paths exist which are not shown in the diagram in the appendix, for clarity.

The *star topology* assumes that each node in an area has direct connection to the data concentrator in its area. This data concentrator can be at a substation or it can be a special node. Measurement data is directly transmitted to the data concentrator which in turn passes it on to the control center. This topology undoubtedly leads to faster data communication but it is costly since it involves dedicated links to each substation. The right of way available from the power transmission system may not be adequate for this communication network topology and additional right of way might be needed for the communication links.

Figs. A.2 & A.3 in the Appendix show schematic diagrams of the communication topologies used for this work.

3.3 Special Protection Scheme

An introduction to the Special Protection Scheme (SPS) is given in chapter 1. It should be pointed out here that the abbreviation SPS actually expresses only one function of the wide-area control systems. A wide-area system may be a platform serving various purposes. It acquires data (measured synchronously) and communicates them into one central location where they can be processed. The use of this data may include:

- Wide area monitoring – the system can offer very accurate information (synchronized measurements with a high sampling rate) about the states which would not be otherwise observable, such as oscillations, load dynamics etc. (the displayed quantities may range from power flows, magnitudes and phase angles

of voltages and currents to stability indicators).

- Wide area protection – SPS in traditional, conventional understanding. In case of situations endangering the power system (detected incipient instability), SPS executes a single action.

- Wide area control – the system continuously, after the recognition of a state prone to instability, influences the behavior of the power system to follow a certain trajectory to avoid instability and keep the power system within safe boundaries. A feedback control loop is employed to do so.

- Wide area optimization – there are two interpretations of this term. Both of them are basically economical in nature and aim at the operation of the network in the most profitable way. The first one, minimization of losses and similar tasks are usually done by Energy Management Systems. The other one expresses possibility to fully utilize the network, i.e. operate it close to its limits, what is allowed by above mentioned wide area control, thus implicitly fulfilled by it.

For the system in this work, two cases of system instability were obtained for which control algorithms have been determined to generate protection or control signals to prevent the system from going unstable.

Case 1: In this case the system shows transient angle instability following the fault. The generator angles separate into two groups and start moving apart. There is a clear indication of system separation. The SPS scheme determines the angle of separation between the groups of generators and separate the area into islands, if it exceeds a pre-specified value. Load and generation are balanced in the each of the islands following separation.

Case 2: This case shows oscillatory instability. Angles of the generators exhibit undamped oscillations of low frequency. The generator angle and frequency plots

shows increasing oscillations. The SPS scheme detects the growing oscillation and reschedules the generation in the system. Such a scheme have been successfully applied by Chung *et al.* in [20]. However, it was found that generation rescheduling by itself was not a sufficient control measure to restore stability. Additional control action, to reduce the power system stabilizer gain (K_{STAB}), if the stabilizer output hit its limits (V_{Smax}/V_{Smin}), had to be taken.

Chapter 4

Simulation Approach

In an electric power system, energy flows from bus to bus via the network. The dynamics of each machine, $\delta(t)$, are influenced by this energy flow through the P_g term in the differential equation of motion of the machine rotor. The specific terms in P_g which correspond to this coupling are δ and V [21]. At each machine, energy is transferred to the network depending on the machine bus voltage magnitude and phase. These voltages are influenced by the network parameters and are essentially in the sinusoidal steady state. Usually, the electromagnetic behavior during the very short period directly following the disturbance is not required. Therefore, the assumption of instantaneous network response is adequate.

4.1 The Dynamic Simulation

The starting point for any power system dynamic simulation program is the pre-disturbance power flow solution. The system is always assumed to be in a steady state when the initiating disturbance occurs. The steady state simulation is done to check for the integrity of the input data. This is shown in the loop marked 'Steady State Simulation for Data Check' in Fig. 4.1. As a result, using the pre-disturbance power flow solution, all the initial values of the state variables that govern

the differential equations are calculated. After these are obtained, the disturbance is simulated by changing the bus admittance matrix shown in **Step 8** of the flow chart. The simulation of the disturbance causes a mismatch between the mechanical power input to the generators and electrical power output of the generators. Hence, the equilibrium is upset, and the values of the state variables governed by the various differential equations coupled with the algebraic equations change. This change is tracked by numerically integrating the coupled set of differential and algebraic equations (**Step 12**). The time evolution of the state variables and other system variables is observed to determine the behavior of the system.

The overall system equations, including the differential equations for all the devices and the combined algebraic equations for the devices and the network, describing the mathematical model of a mutimachine power system is given in Chapter 2. Time-domain simulation of the system dynamics is done by solving these equations at each time-step. A wide-range of numerical approaches has been reported in the literature for solving these equations, depending on the numerical methods and the modeling details used [5, 21, 23, 24]. Ref. [22] provides a review of these approaches. The many possible schemes for the solutions of the differential-algebraic equations are characterized by the following factors:

- The manner of interface between the differential equations and the algebraic equations. Either a *partitioned* approach or a *simultaneous* approach may be used.
- The integration method used, *i.e.,* implicit method or explicit method.
- The method used for solving the algebraic equations. As in power flow the following methods may be used:
  - the Gauss-Seidel method based on admittance matrix formulation,
  - a direct solution using sparsity-oriented triangular factorization, and

– an iterative solution using the Newton-Raphson method.

All of the above approaches/methods have been successfully used in production grade programs. In this program, solution of the differential-algebraic equations was done using the partitioned approach. The fourth-order Runge-Kutta integration algorithm was used. This an explicit integration method. The MATLAB function *ode45*, which employs the fourth-order Runge-Kutta algorithm for numerical integration, was used. This function automatically chooses the integration time-step depending on the dynamics of the state variables.

To prepare the system data for a stability study, the following preliminary calculations are made:

1. The system data are converted to a common system base, a system base of 100 MVA was conventionally chosen.

2. The load data from the prefault power flow are converted to equivalent admittances. The necessary information for this step is obtained from the result of the power flow. If the voltage at a certain load bus is V, the equivalent impedance at the load bus is,

$$Y_{eq} = (A_1 P_0 - jB_1 Q_0)/V_0^2 + (A_2 P_0 - jB_2 Q_0)/V_0 V + (A_3 P_0 - jB_3 Q_0)/V^2 \quad (4.1)$$

   where, the nominal complex power demand at the load bus is $P_0 + jQ_0$ at a nominal voltage V_0, and the constant impedance, constant current and constant power components are A_1, A_2 & A_3 for real power and B_1, B_2 & B_3 for reactive power, such that $A_1 + A_2 + A_3 = B_1 + B_2 + B_3 = 1$.

3. The internal voltages of the generators $|E|\angle\delta = E_d + jE_q$ are calculated from the power flow data using the predisturbance terminal voltages $|V|\angle\theta$ using,

$$|E|\angle\delta = |V|\angle\theta + (R_a + jX_q I) \quad (4.2)$$

   I is obtained from the bus power injection and bus voltage.

4. The prefault augmented Y_{bus} matrix is calculated. To obtain this, the equivalent load admittances calculated in step 2 above, are connected between the load buses and the reference node (ground). Additional nodes are provided for internal generator nodes and the appropriate values of admittances corresponding to $X_d^{'}$ are connected between these nodes and the generator terminal nodes.

5. In the final step we eliminate all the nodes except the internal generator nodes using *Kron reduction*. After Kron reduction we obtain the reduced Y_{bus} matrix $\hat{Y}$ [24]. This matrix has a dimension $(n \times n)$, where n is the number of generators.

The heart of the program is the main simulation loop shown as 'Dynamic Simulation Loop' in the flow chart in Fig. 4.1. Here, the solution of the differential and algebraic equations are obtained at each time-step and the state variables are updated. This loop is implemented in the program by calling the MATLAB *ode45* function with a start time, an end time, and the initial values of the state variables for this interval. This function uses the MATLAB script or function file, which contains the differential equations, to get the values of the derivatives at each time-step. The function is designed to choose a time-step depending on the dynamics of the state variables.

To implement relay checking routine, another feature of the *ode45* function called *OutputFcn* was used. This function is called at the end of each time-step by *ode45*. The system variables are checked here for their limits. This is illustrated in (**Step 13** in Fig 4.1). If any breaker/recloser or special control action is required, the output status of this function changes to '1' and the program exits the integration loop. This is shown in **Step 16** of the flow chart. For breaker/recloser, timers are set according to the relay settings. But for a wide-area control action due to the Special Protection Scheme, the communication delay for the specific action is determined

(**Step 17**). The pending action for the current time is then performed (**Step 18**) and the time interval for the next call to the *ode45* routine is updated (**Step 19**). The start time is set as the time where the previous *ode45* call exited. The end time is the most urgent of the action time of all pending breaker/recloser. The final values of the state variables from the last call to the function are used as the initial values for the next call.

Simulation of the Special Protection Scheme is also done using the *OutputFcn* feature of *oder45*. Similar to implementation of relays, the SPS logic is applied on the system variables and control action, if any required, are determined (**Step 14**). This is done at each time-step. The program can be modified to do this operation every t secs., instead of every time-step. This t can be user-specified. However, in an actual system, the SPS logic unit is located at the control center. This involves communication of measurement data from the substations to the control center and that of control signals from the control center to the devices at the substations. Thus, control actions due to the SPS has to be simulated taking the communication delays into account.

4.2 Simulation of the Communication System

Data communication involves various types of delays. Although for fiber-optic communication channels the propagation delay is almost negligible, the delays due to queuing and processing can be significant and may have a pronounced impact on system stability. For determining wide-area control actions measurement data from various locations in the network is required. Communication of data from different locations experience different amount of delays before they reach the control center. For the purpose of SPS, these data from various locations needs to be synchronized in time. Schemes like GPS time-stamping of data, etc are used in practice.

For the purpose of this program, two different topologies for communications

were assumed. The effects of these on system response for the test cases was observed. The delay-data for them were used to pre-calculate the net delay to send signals from various substations to the control center. The signal paths were also pre-assumed. Synchronisation of data from various locations is simulated by using the maximum of the delays of all the input measurement data, required for the processing and control decision, as the net delay for communication of data from substation to the control center. This is then added to the processing and decision-making time at the control center and the communication delay from the control center to the substation for the control signal. However, in the simulation program the measurement data is immediately available to the control center as global variables. Thus the delays are simulated by waiting for the calculated net delay duration before taking any action due to that signal (**Steps 17 & 20**). Failure of a communication link was simulated by making the propagation delay for that link to be a very high value (more than the total simulation time).

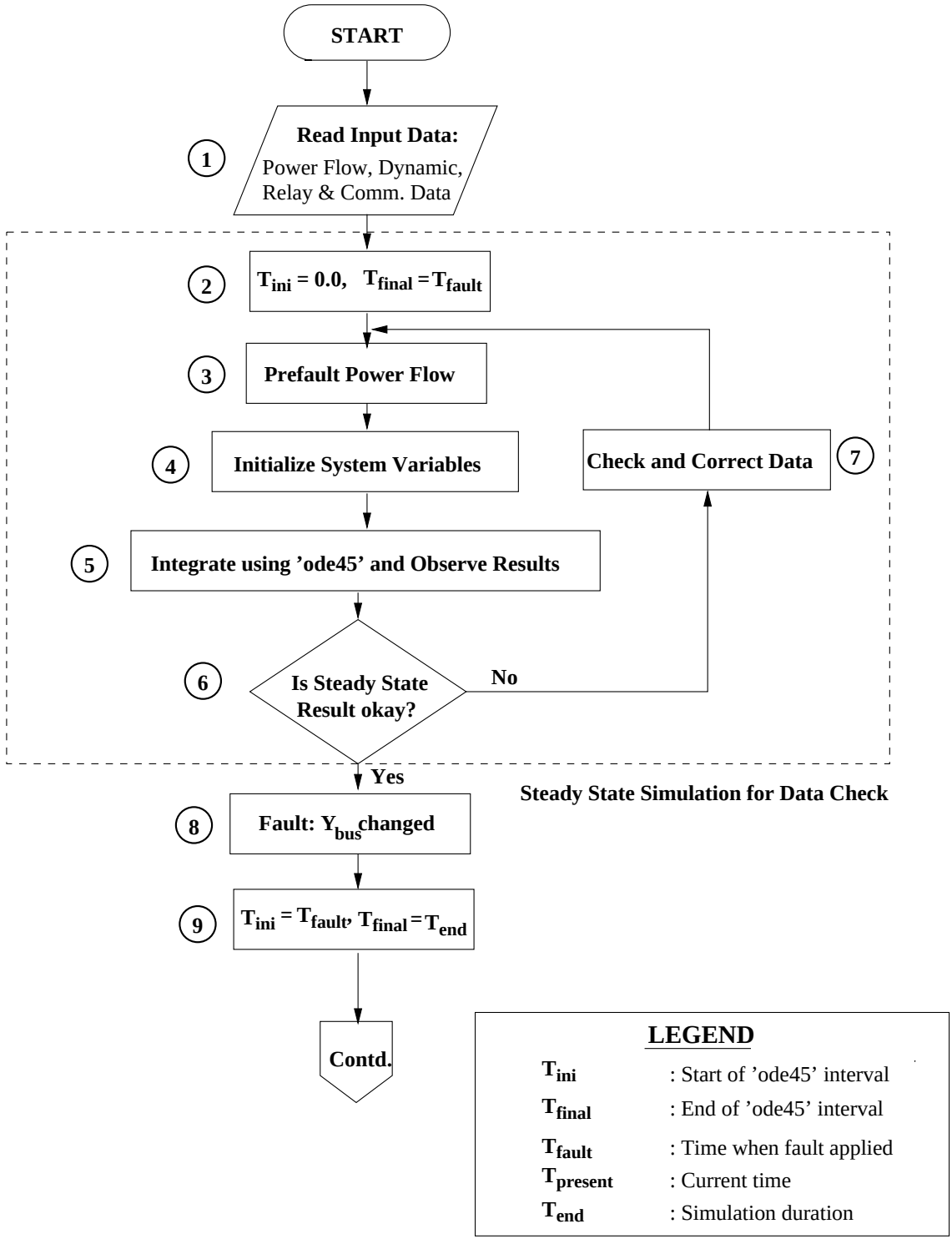

Figure 4.1: Simulation Flowchart

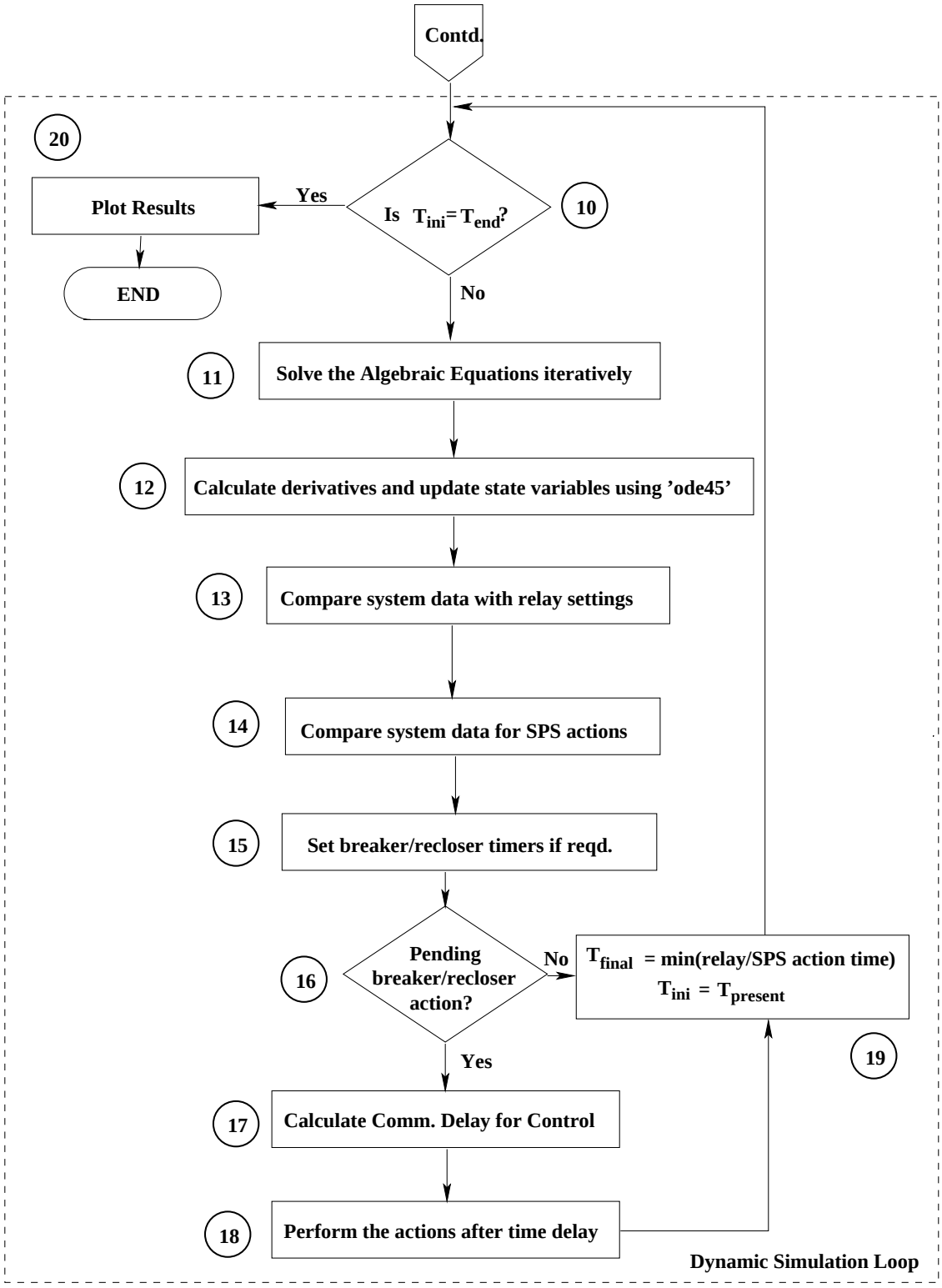

Figure 4.1: Simulation Flowchart(cont'd)

4.3 Typical Sequence of Events

The program written for this work incorporates relays, circuit breakers, wide-area measurement & control and communications. Thus, a typical sequence of events for this program would be:

1. Normal system operation (Steady State).
2. Fault occurs at some place in the system.
3. Fault or abnormal system condition detected by the protective relays.
4. Breaker or switching actions taken (Usually local actions).
5. If these local actions are inadequate for system stability, additional wide-area control actions like generation changes or exciter/PSS controls initiated. This involves the communication system which transfers measurement data to the control center and control/trip signals from the control center to the devices.
6. Restoration of stable operation.

Steps 3, 4 and 5 may occur repeatedly until system is restored to an acceptable state of operation. Most WACS control actions are discrete feed-forward controls. The local relay transducers (CTs and PTs) are active throughout the simulation so that multiple contingency or cascade event can be monitored and controlled. Wide-area measurement & control systems may or may not be active throughout the simulation. Certain special protection schemes, which are a part of the wide-area measurement & control system, are active only during particular system conditions.

Chapter 5

Results and Discussions

The programs written, were tested for stability studies of the IEEE 39-bus system. The base case power flow data and the component parameters for this system are given in Appendix A. The system diagram is shown in Fig. A.1 in Sec. A.3. Two test scenarios of instability were generated. This was done by increasing the stress on the transmission system by increasing generation in one area and increasing an equal amount of load in some other area. A three-phase fault was then applied on a transmission line and the response observed. These scenarios are described in the following sections.

5.1 Scenario 1: Separation of Area

5.1.1 Unstressed System

For the case of a balanced, three-phase, 6-cycle fault on line 16-17, the post fault system is found to be stable with line 16-17 removed. Here, by line 16-17 is meant, the transmission line from Bus 16 to Bus 17. The load and generation values for this case was the same as those given in the power flow data in the Appendix. The angle plot for this stable case is shown in Fig. 5.1. Since the subsequent swings for

all the generators are decreasing we can conclude that the system is transient stable.

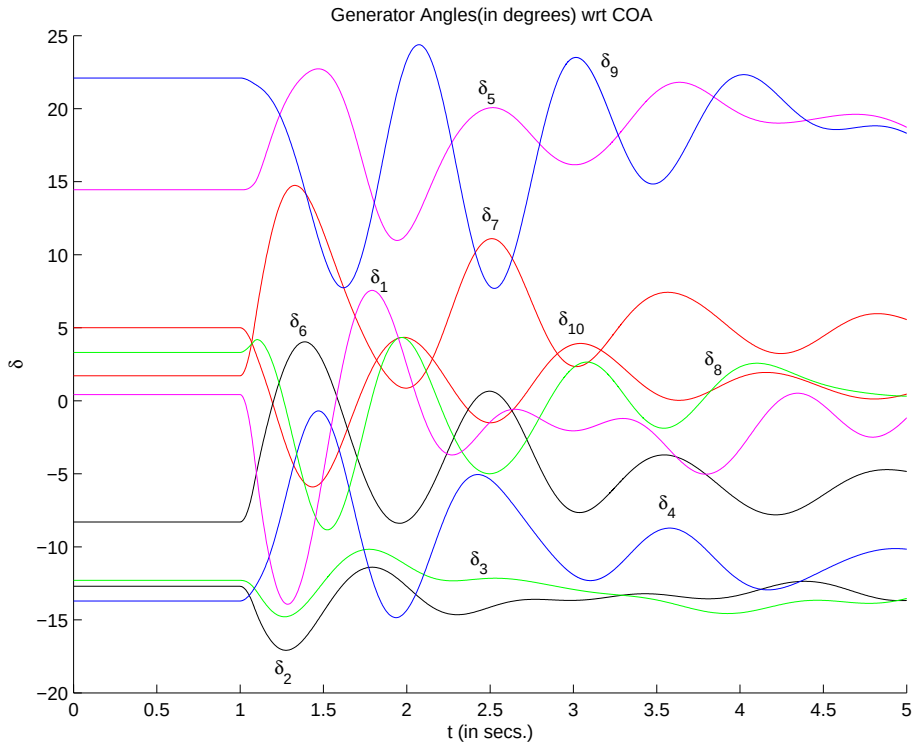

Figure 5.1: Unstressed System: Transient Stable

5.1.2 Stressed System without any SPS action

To obtain a case of instability, power flow on the line 16-17 was increased. This was done by increasing the power generated at generators 4, 5, 6 and 7 by 25% and increasing real and reactive loads at buses 18, 25, 26, 27, 28 and 29 by 45%. The total increase in generations and loads was such that net power balance was maintained. In other words, the amount of increase in generation and load was equal. The same fault conditions, as described above, on the stressed system revealed that the system goes unstable. Interarea separation can be clearly witnessed as shown in Fig. 5.2. Following the fault, the angles of generators 4, 5, 6 & 7 starts increasing whereas those for generators 1-3 & 8-10 starts decreasing. The angle trend for generators 2

& 3 differs slightly from those of the other in the group. This can be explained by the fact that these two generators are located away from the other four and are less tightly coupled to them as they are among themselves.

A comparison of the plots of the generator angles for the stressed and unstressed cases for a 1.6 sec. simulation time is shown in Figs. 5.2 & 5.3. The generators angles shown in Fig. 5.3 for the unstressed case, are disturbed from their steady state values, when the fault was applied at 1 sec. But after clearing the fault at 1.1 sec. the generator angles stabilize. On the other hand, for the case when the same fault is applied on the stressed system, the generator angles increase or decrease monotonically as seen from their plots in Fig. 5.2. Thus the case with the fault on the unstressed system is transient stable whereas the latter one wit ht he same fault applied on the stressed system is unstable.

5.1.3 Stressed System with SPS action

For the above case of interarea separation, a special protection scheme was devised to island the system into the two areas. This scheme involved wide-area angle measurement from all the generator units. Derivatives of the angles were obtained from the time measurements and angle trend determined from these derivatives. Generators were grouped according to the sign of their derivatives (positive or negative implying increasing or decreasing angles) and the averages of the angles in the separating groups were compared. If the difference in average angles of the two groups was greater than a specified value (In this work: 70°), the areas were separated by deliberate control action. For this case, Line 15-16 and line 16-17 were required to be tripped for islanding the separating areas. Since line 16-17 was already tripped by the zone–1 relay following the fault, only line 15-16 has to be tripped. It should be noted here, that a system islanding involves matching load and generation in the islands created. For this test case, this was accomplished by tripping generator

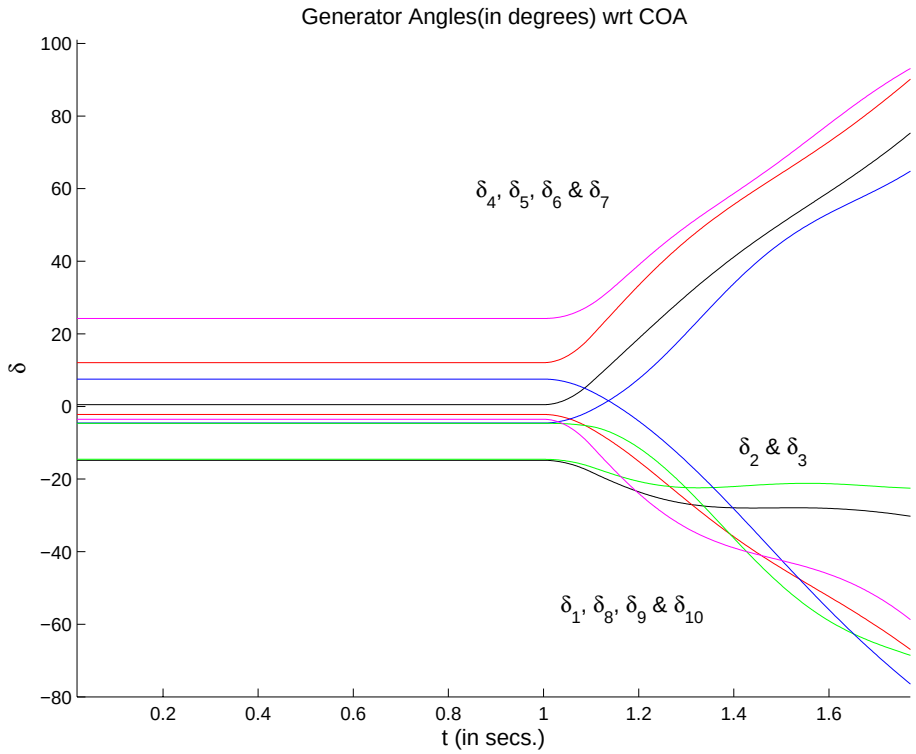

Figure 5.2: Stressed System: Without any SPS control action shown monotonically increasing or decreasing angles

6 and putting a resistive brake on Bus 20 for the island with over generation and decreasing the load at Bus 39 for the island with overload.

It is quite obvious that the special protection scheme described above involves wide-area communication. Measurement data (generator angle data in this case) at the substations (all the buses in this system are assumed to be substations, where data is being measured) had to be communicated to a central location for system analysis, and control signals (line trip for islanding etc in this case) sent to the remote locations where the controllers/breakers are located.

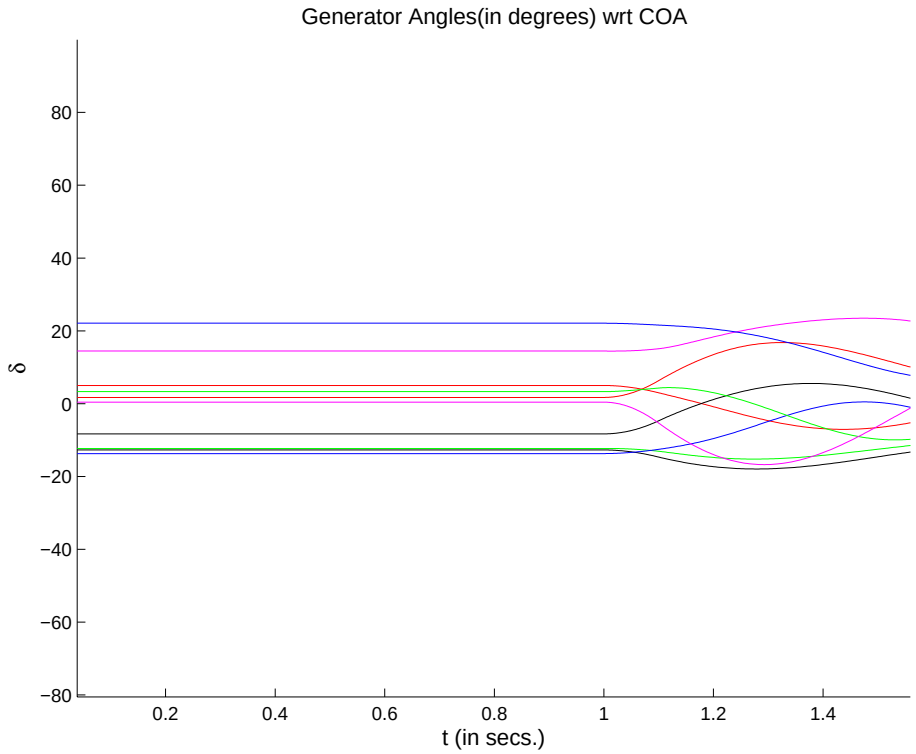

Figure 5.3: Unstressed system: 1.6 secs simulation to compare with Fig. 5.2 for stability

SPS using Mesh Topology for Communication

The effects of communication delays on stability were studied for both the communication topologies described earlier. For this topology the communication delays were calculated based on the number of hops a signal has to encounter to reach the control center. The delay values for data measurement, propagation, concentrator throughput were taken from [19]. Propagation delay was multiplied by the number of hops. The generator angle plots for the SPS scheme using a mesh communication topology is given in Fig. 5.4. These results illustrate, that the communication delays arising out of the mesh topology are so high that system instability could not be avoided. This is expected, because transient stability demand a very fast

control action, which a mesh topology could not provide. The star topology for communication gave cases of stability and was investigated further.

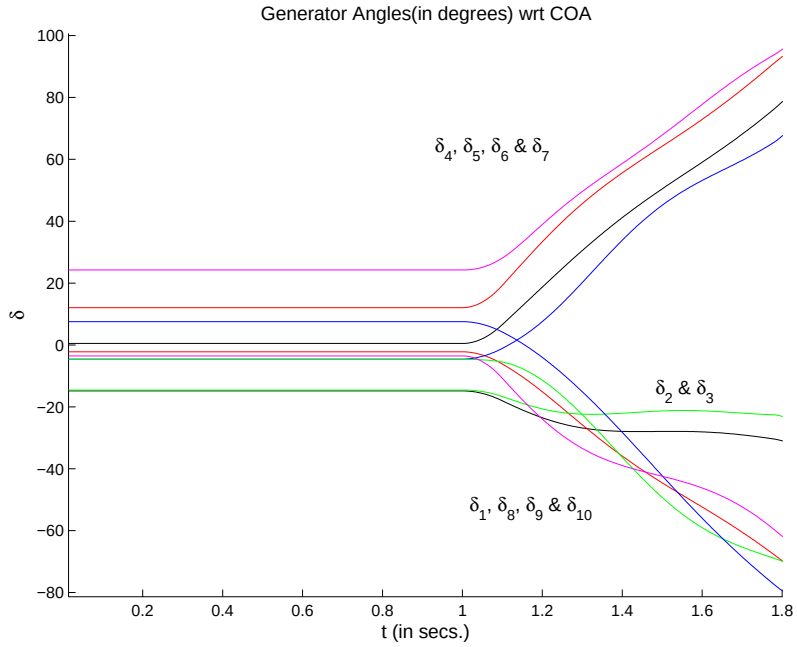

Figure 5.4: Stressed system with SPS: Using the mesh topology the system is unstable

SPS using Star Topology for Communication

Using the star topology for communication, the system is found to be stable. The system is islanded by the SPS early enough to ensure stability and minimal loss in terms of generation loss or load shedding. The maximum delay that the communication can endure before further generation loss occurs is 153 ms. The generator angle plots for the two islands for this case with no link failure is shown in Figs. 5.5 & 5.6. The angles in the two areas are plotted with respect to their centers of angle, which are the averages of the angles in those areas. In Fig. 5.6, δ_6 becomes zero after the SPS action is taken, which indicates that generator 6 has been tripped.

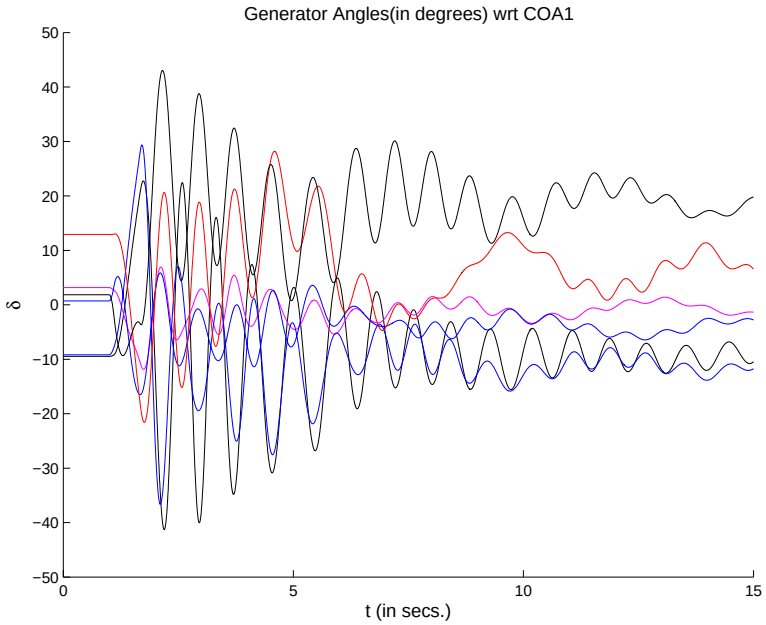

Figure 5.5: Area 1 with SPS action using the star topology: All SPS control signal delays are 153 ms or less

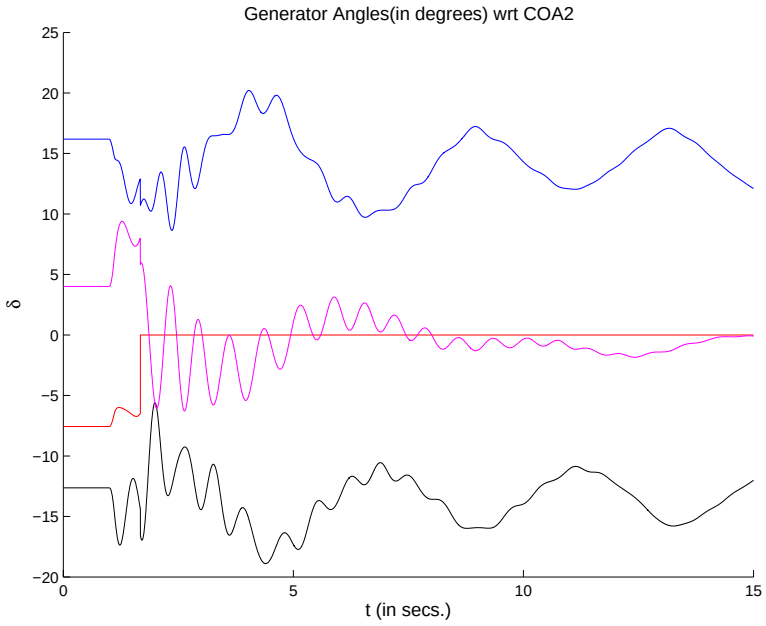

Figure 5.6: Area 2 with SPS action using the star topology: All SPS control signal delays are 153 ms or less

Star Topology: Large delay in Line Trip (islanding) signal:

Further simulation with different delays showed that to ensure stability and/or a minimum loss of generation and subsequent loads, the delay in the line-trip signal to island the system is critical. Excessive delay or failure in the line trip signal leads to instability. Using a uplink delay time of 116.67 ms or 7 cycles to communicate measurement data to the control center, and processing time of 1 ms, if the communication delay to trip the line is more than 153 ms, no matter what the delay for the other SPS control signals are, generator 2 is lost due to overfrequency. Generator angle plots for the two islanded areas are shown in Figs. 5.7 & 5.8. These plots reveal that although the areas might be stable after islanding, the loss of an extra generator along with load is witnessed which is not desirable. For higher delay, the results are worse with more generator trips due to over/under frequency.

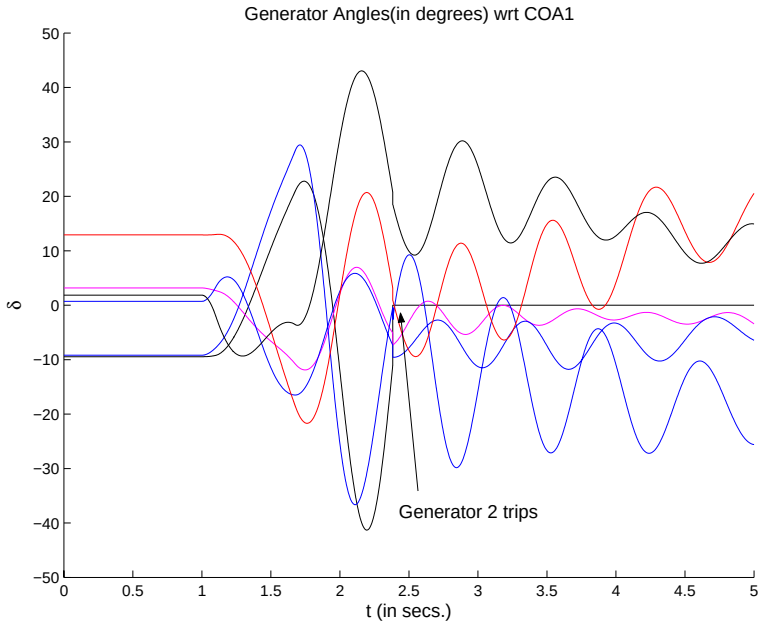

Figure 5.7: Area 1 with SPS using star topology: Line trip delay is 155 ms. All other control signal delays are 153 ms

Star Topology: Large delay in Generator/Load Trip signal:

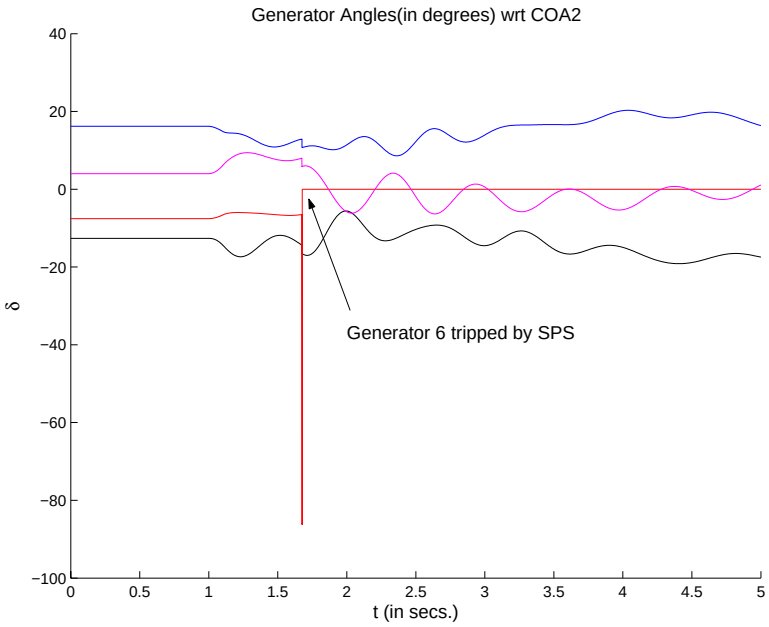

Figure 5.8: Area 2 with SPS using star topology: Line trip delay is 155 ms. All other control signal delays are 153 ms

If the line trip delay is within 153 ms, then the maximum delay that the generator and load trip signal can endure, so that no further generation and load is lost, is 216 ms. A case of this delay being 220 ms leading to trip of generator 2 & 7, is shown in Figs: 5.9 & 5.10. Here we see that, due to this extra delay in the SPS control signal that tries to match the generation and load in the islands there is further loss of generations and loads. Besides tripping of generator 6 by the SPS action, Area 1 loses generators 1 and 2 and Area 2 loses generator 5. Since generator 1 is a big generating plant in the system, its loss is particularly undesirable.

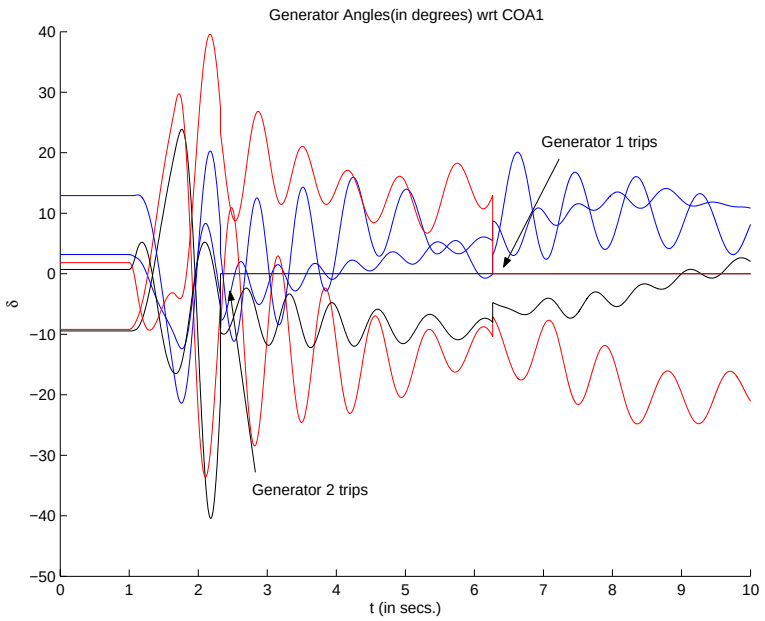

Figure 5.9: Area 1 with SPS using star topology: Line trip delay is 153 ms. Other control signal delays are 220 ms

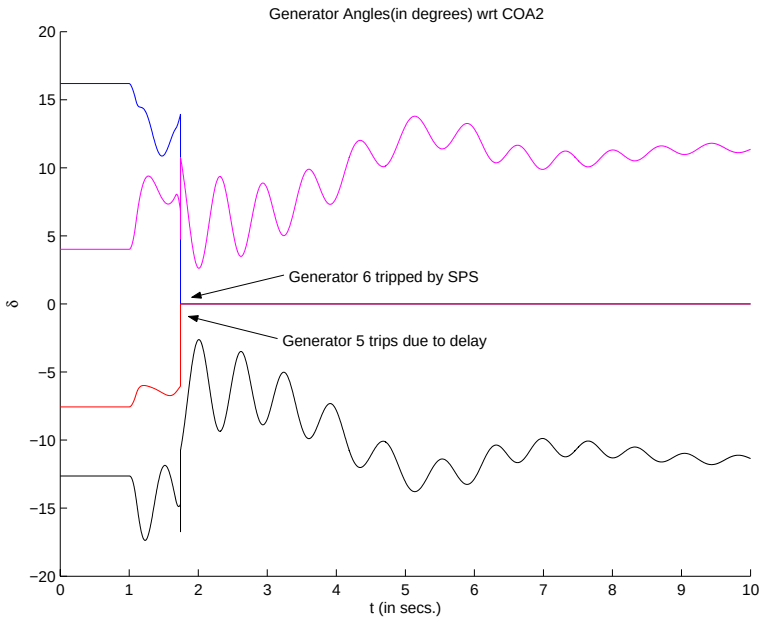

Figure 5.10: Area 2 with SPS using star topology: Line trip delay is 153 ms. Other control signal delays are 220 ms

Star Topology: Loss of Resistive Brake Switching Signal:

A case of loss of communication signal to switch on a resistive brake in area two after islanding is shown in Figs. 5.11 & 5.12. This case leads to instability in area 2 where all the generator are eventually tripped, as witnessed in the generator angle plots for Area 2. However the machines in Area 1 are all stable.

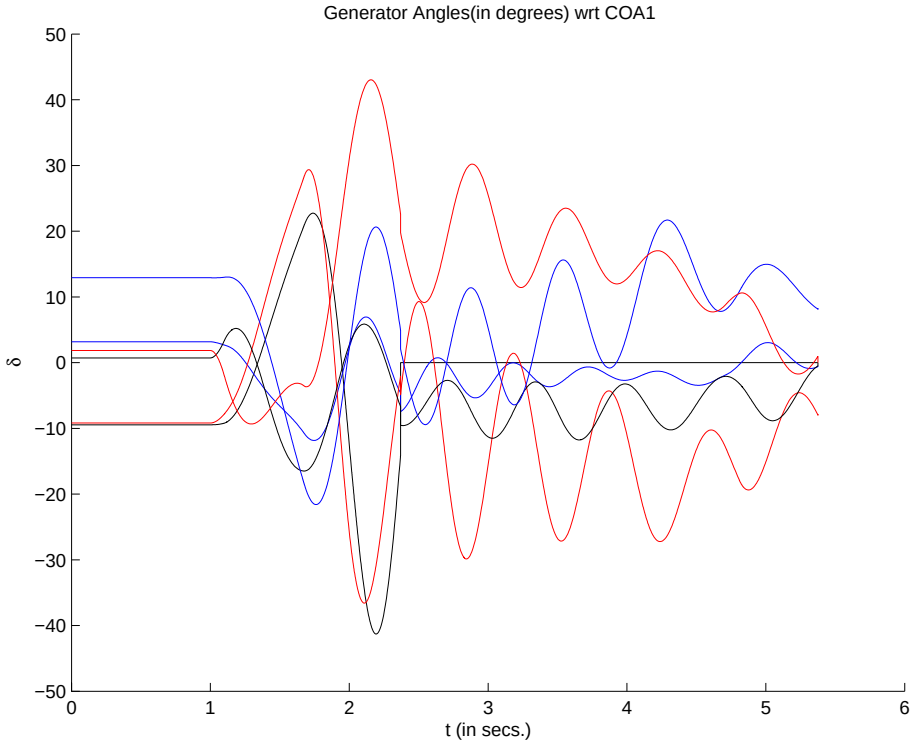

Figure 5.11: Area 1 with SPS using star topology: Failure of communication signal to switch in the resistive brake on bus 20. All other control signal delays are 153 ms.

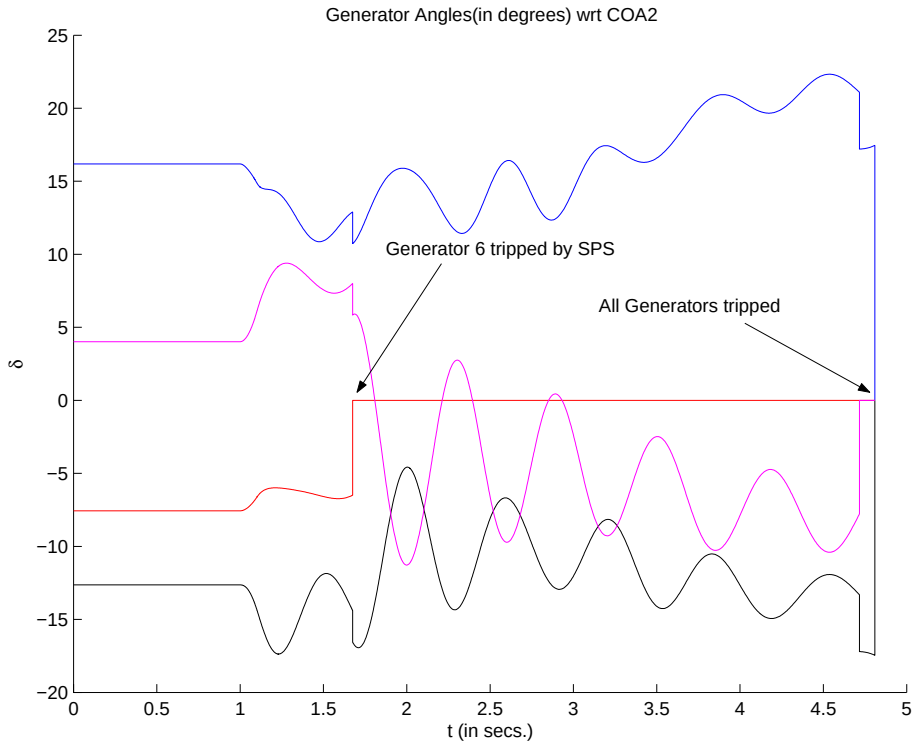

Figure 5.12: Area 2 with SPS using star topology: Failure of communication signal to switch in the resistive brake on bus 20. All other control signal delays are 153 ms.

5.2 Scenario 2: Oscillatory Angle Instability

5.2.1 Unstressed System

Cases of oscillatory instability were obtained by increasing the power generated at generators 8, 9 and 10 by 35% and real and reactive loads at buses 7 and 8 by 75%. A balanced, three phase, 3 cycle fault on line 4-5 was applied. As in the previous case, the post-fault system is found to be stable if the system is not stressed *i e.*, if the generations and loads are not increased from their base case values. The generator angle plots for this case are the same as shown in Fig. 5.13.

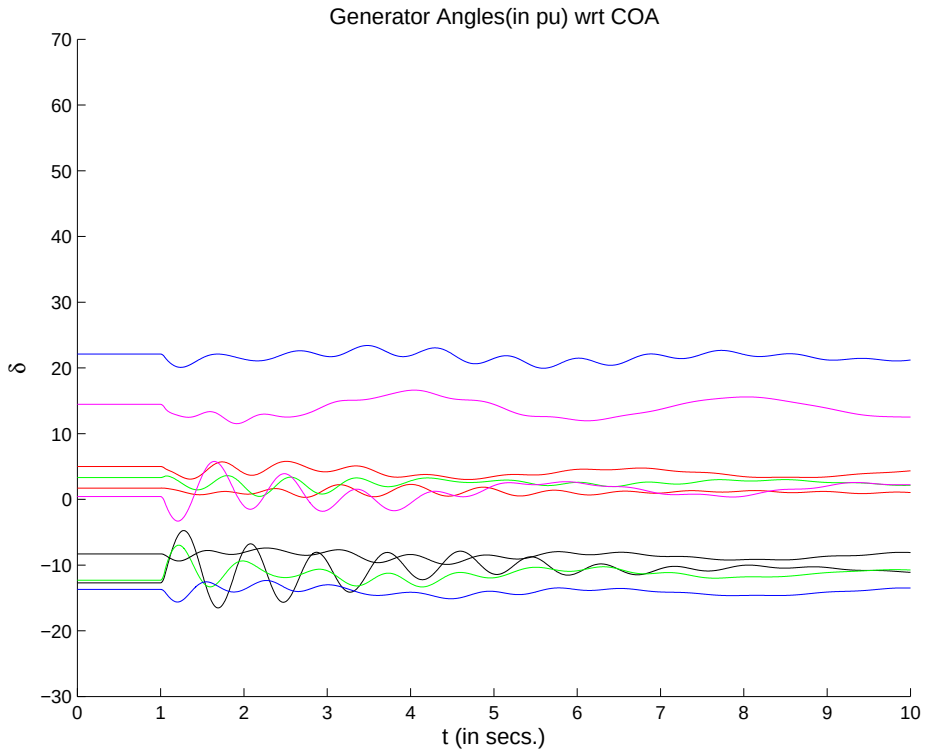

Figure 5.13: Unstressed System for scenario 2: Stable

5.2.2 Stressed System without any SPS action

Post fault simulation of the stressed system reveal a case of oscillatory angle instability, where generator angles show undamped oscillations of low frequency. This trend is system-wide with all generators exhibiting this behavior. Fig. 5.14 shows the generator angle plots for this case.

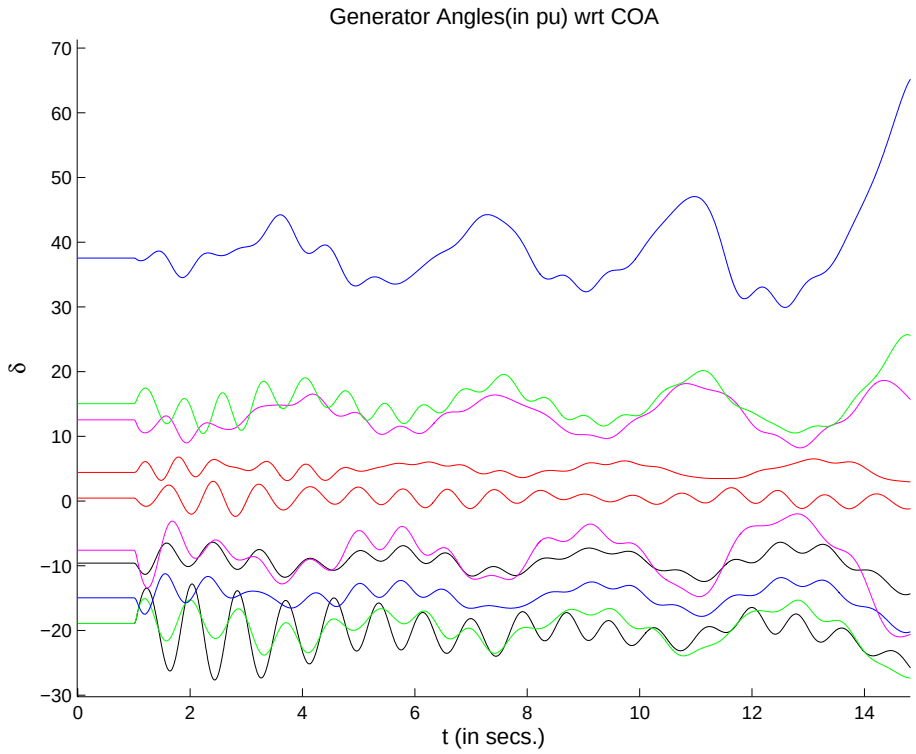

Figure 5.14: Stressed System without SPS action showing growing oscillations for almost all machines.

5.2.3 Stressed System with SPS action

The special protection scheme for this case involved rescheduling of generations in the system. Generations of units 8, 9 and 10 were reduced by 10% and those of 2 and 3 were increased by 18%. It was found that mere rescheduling of generation

was not enough to stabilize the system. Higher amount of rescheduling had no significant effect on the response. So another SPS scheme was armed following the detection of the unstable oscillations. The output of the power system stabilizers were monitored and if they hit any of their specified limits (V_{Smax} or V_{Smin}), the respective stabilizer gains (K_{STAB}) were reduced. This scheme along with generation rescheduling stabilized the system, as seen from the plots in Fig. 5.15.

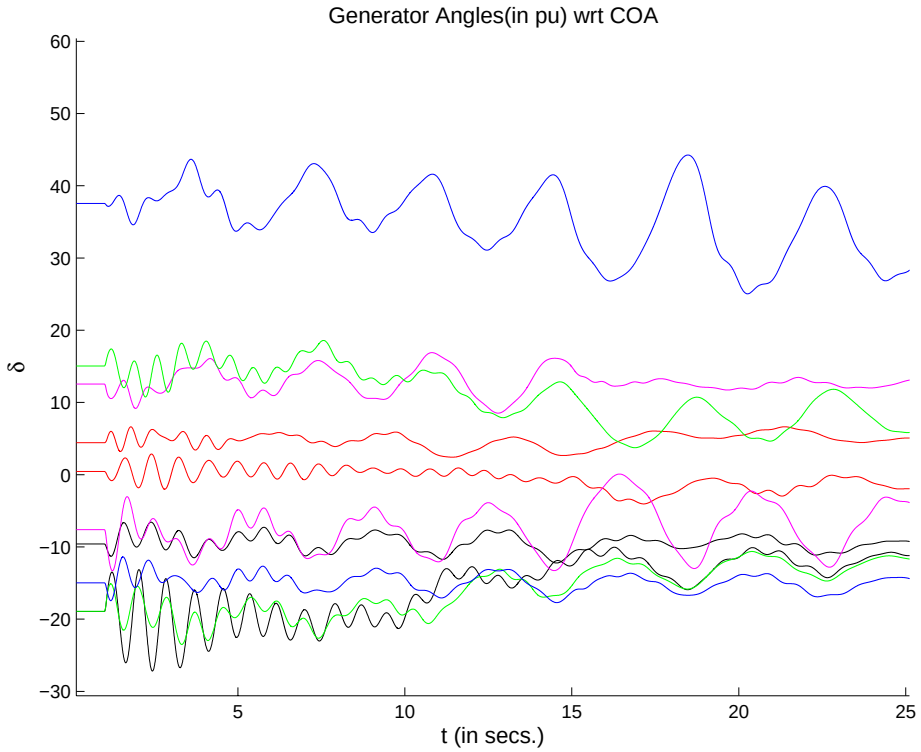

Figure 5.15: Stressed System with SPS action shows growing oscillations damps after SPS control actions were taken

Case of Loss of Control Signal:

It was also observed, that, for this scenario of oscillatory instability, more time is available for control actions. Using either of the communication topologies (mesh or star), the controls could successfully stabilize the system. Only the case of a communication link failure led to system instability. Such a case, where a stabilizer gain could not be decreased due to lost control signal is shown in Fig. 5.16. The plots show that the angle oscillations for some generators keeps on growing. Generator 9 finally trips due to overfrequency. The frequency plots of the machines for this case is shown in Fig. 5.17.

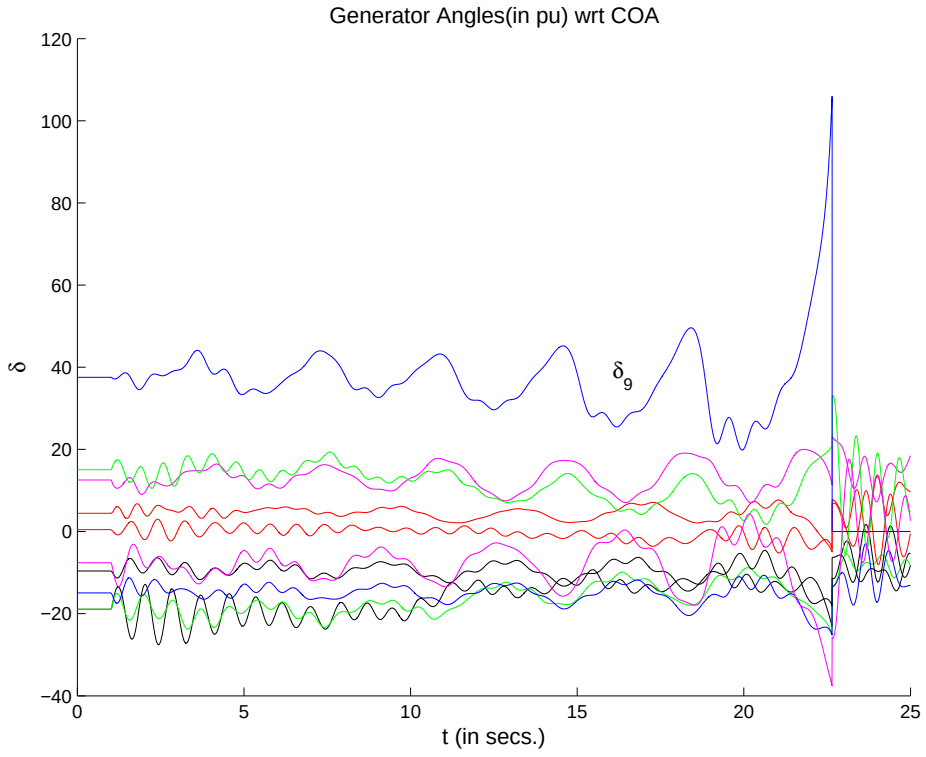

Figure 5.16: Case of communication failure of SPS signal to change stabilizer gains. Generator angle plots

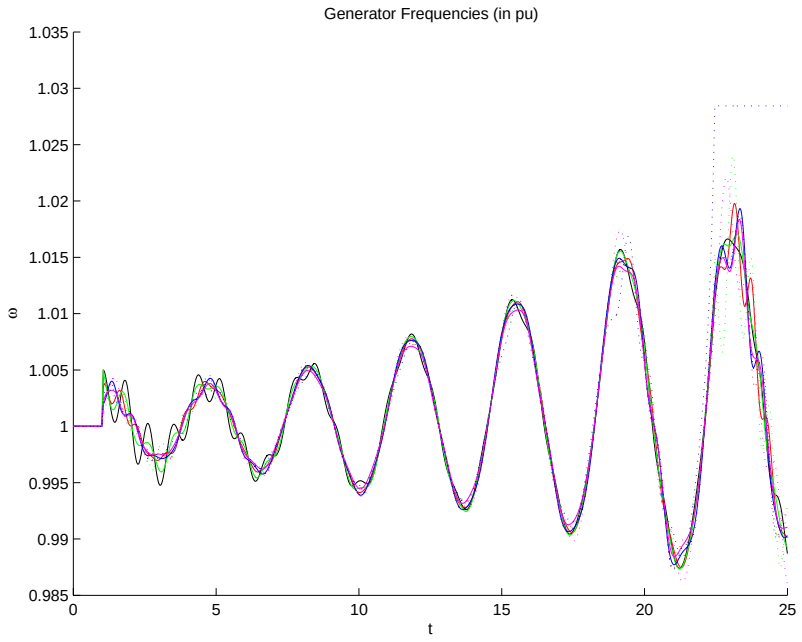

Figure 5.17: Case of communication failure of SPS signal to change stabilizer gains. Generator frequency plots.

Chapter 6

Conclusions and Future Work

A software tool to study the effects of communication network for measurement and control signals on power system behavior was developed. Wide-area control schemes, including special protection schemes, can be studied using this tool. As required by the scope of this work, protective relay models were also included with other system components. Once the program was ready, system dynamic studies were performed choosing the IEEE 39-Bus system as the test system. Cases of instability were generated for which local protection relays were insufficient to protect/stabilize the systems. Hence, different special protection schemes and control were tried and schemes specific to the cases were determined. Following this, the effect of communication delays was studied. For this, two different communication topologies were implemented and the effects of delays inherent in them were studied for both the cases.

6.1 Conclusions

As seen from the results in the last chapter, communication topology and delay has got a significant effect on the dynamic response of a power system. This is specially true in contingency situations where the communication networks are used to relay

control signals to the devices. However communication delays are equally important for transmitting measurement data to the control center. As seen in the scenario for transient stability, the mesh topology was unable to stabilize the system because the delay in sending the measurement data from the substation to the control center was quite high. The fact that delays were less important for the case of oscillatory instability can be used to set up control signal priorities in communication. Control signals to avoid transient stability can be given higher priority for communication through the network.

This simulation program has proved to be an elegant tool for such studies and forms a basis for developing commercial-grade dynamic simulation software with diverse capabilities.

6.2 Future Work

Although the programs written for this work satisfies the scope of the project, the work doesn't end here. This work was not intended to be just a mere study program in MATLAB but to be a prototype for a commercial-grade software that can model communication and control into power system dynamic simulation. To that effect this work calls for further developments to the program, some of which are enumerated below:

1. The data for the system has been typed-in manually into the program. A parser to read data in standard formats like PTI or CDF is required.

2. The programs for this work has been written in MATLAB. The simulation time required is very high. Even for such a small test system, it takes almost 20-25 times the real time to simulate. One reason for this is that the routines in MATLAB used for this work are not all optimized for this application. Hence, coding this program in some other language like C/C++ will improve

the simulation time to a large extent.

3. A user-friendly Graphical User Interface, without taxing the computational time requirement of the program, is required.

4. The model for the communication network could be improved with the delays being an output of the model rather than its parameters.

Appendix A

Test System Data

The IEEE 39-Bus system was used as the test system for this work. This Appendix contains the relevant data for this system. The single-line diagram of this system is given in also included Fig. A.1.

A.1 Power Flow Data

The power flow data for this system is divided in:

- Bus Data
- Load Data
- Generation Data
- Branch Data

Bus Data

Table A.1 represents the bus data. The nomenclature for the table headings is:

Bus Number	Number of the bus (1 to 39)
Bus Name	Alphabetic identifier for each bus
Bus BaskV	Bus base voltage, in KV

Bus Type	Bus type code:
	(1) Load Bus. PQ bus
	(2) Generator Bus, PV bus
	(3) Swing Bus
Bus G_L	Real component of shunt admittance to ground, in MW
Bus B_L	Reactive component of shunt admittance to ground, in MVAR
Bus Voltage	Voltage magnitude, in per unit
Bus Angle	Voltage angle, in degrees

Table A.1: IEEE 39-Bus Test System: Bus Data

Bus Number	Bus Name	Bus BaskV	Bus Type	Bus G_L	Bus B_L	Bus Voltage (pu)	Bus Angle
1	BUS1	345	1	0.0	0.0	1.04814	-9.4266
2	BUS2	345	1	0.0	0.0	1.05050	-6.8854
3	BUS3	345	1	0.0	0.0	1.03411	-9.7286
4	BUS4	345	1	0.0	0.0	1.01161	-10.5291
5	BUS5	345	1	0.0	0.0	1.01647	-9.3765
6	BUS6	345	1	0.0	0.0	1.01725	-8.6816
7	BUS7	345	1	0.0	0.0	1.00668	-10.8417
8	BUS8	345	1	0.0	0.0	1.00570	-11.3376
9	BUS9	345	1	0.0	0.0	1.03220	-11.1509
10	BUS10	345	1	0.0	0.0	1.02346	-6.3140
11	BUS11	345	1	0.0	0.0	1.02012	-7.1235
12	BUS12	345	1	0.0	0.0	1.00721	-7.1351
13	BUS13	345	1	0.0	0.0	1.02066	-7.0184
14	BUS14	345	1	0.0	0.0	1.01808	-8.6628
15	BUS15	345	1	0.0	0.0	1.01937	-9.0593
16	BUS16	345	1	0.0	0.0	1.03457	-7.6558
17	BUS17	345	1	0.0	0.0	1.03648	-8.6478

Table A.1: IEEE 39-Bus Test System: Bus Data

Bus Number	Bus Name	Bus BaskV	Bus Type	Bus G_L	Bus B_L	Bus Voltage (pu)	Bus Angle
18	BUS18	345	1	0.0	0.0	1.03427	-9.4855
19	BUS19	345	1	0.0	0.0	1.05086	-3.0390
20	BUS20	345	1	0.0	0.0	0.99142	-4.4475
21	BUS21	345	1	0.0	0.0	1.03373	-5.2570
22	BUS22	345	1	0.0	0.0	1.05085	-0.8181
23	BUS23	345	1	0.0	0.0	1.04588	-1.0161
24	BUS24	345	1	0.0	0.0	1.03986	-7.5361
25	BUS25	345	1	0.0	0.0	1.05869	-5.5136
26	BUS26	345	1	0.0	0.0	1.05359	-6.7740
27	BUS27	345	1	0.0	0.0	1.03990	-8.7842
28	BUS28	345	1	0.0	0.0	1.05091	-3.2666
29	BUS29	22	2	0.0	0.0	1.05048	-0.5097
30	BUS30	22	2	0.0	0.0	1.04750	-4.4697
31	BUS31	22	3	0.0	0.0	0.98200	0.0000
32	BUS32	22	2	0.0	0.0	0.98310	1.6325
33	BUS33	22	2	0.0	0.0	0.99720	2.1762
34	BUS34	22	2	0.0	0.0	1.01230	0.7415
35	BUS35	22	2	0.0	0.0	1.04930	4.1386
36	BUS36	22	2	0.0	0.0	1.06350	6.8297
37	BUS37	22	2	0.0	0.0	1.02780	1.2652
38	BUS38	22	2	0.0	0.0	1.02650	6.5515
39	BUS39	22	2	0.0	0.0	1.03000	-10.9566

Load Data

Table A.2 represents the load data. The nomenclature for the table headings is:

Bus Number Number of the Bus

P_L Real component of the load, in MW

Q_L Reactive component of the load, in MVAR

Table A.2: IEEE-39 Bus Test System: Load Data

Bus Number	P_L (MW)	P_Q (MVAR)
3	322.0	2.4
4	500.0	184.0
7	233.8	84.0
8	522.0	176.0
12	8.5	88.0
15	320.0	153.0
16	329.4	32.3
18	158.0	30.0
20	680.0	103.0
21	274.0	115.0
23	247.5	84.6
24	308.6	-92.2
25	224.0	47.2
26	139.0	17.0
27	281.0	75.5
28	206.0	27.6
29	283.5	126.9
31	9.2	4.6
39	1104.0	250.0

Generation Data

Table A.3 represents the generation data. The nomenclature for the table headings is:

Bus Number	Number of the Bus
P_G	Generator real power output, in MW
P_Q	Generator reactive power output, in MVAR

Table A.3: IEEE 39-Bus Test System: Generation Data

Bus Number	P_G (MW)	P_Q (MVAR)
29	0.00	100.00
30	250.00	136.20
31	572.87	170.34
32	650.00	175.90
33	632.00	103.34
34	508.00	164.39
35	650.00	204.84
36	560.00	96.88
37	540.00	-4.43
38	830.00	19.38
39	1000.00	68.45

Branch Data

Table A.4 represents the branch (transmission lines and transformers) data. The nomenclature for the table headings is:

Number	Number of the branch
From Bus	Branch starting bus number
To Bus	Branch ending bus number
Resistance (pu)	Branch resistance, in per unit
Reactance (pu)	Branch reactance, in per unit
Susceptance (B)	Branch total charging susceptance, in per unit

Branch Tap Transformer off-nominal turns ratio

Table A.4: IEEE 39-Bus Test System: Branch Data

Branch Number	From Bus	To Bus	Resistance (pu)	Reactance (pu)	Susceptance (pu)	Branch Tap
1	1	2	0.0035	0.0411	0.6987	0.000
2	1	39	0.0020	0.0500	0.3750	0.000
3	1	39	0.0020	0.0500	0.3750	0.000
4	2	3	0.0013	0.0151	0.2572	0.000
5	2	25	0.0070	0.0086	0.1460	0.000
6	3	4	0.0013	0.0213	0.2214	0.000
7	3	18	0.0011	0.0133	0.2138	0.000
8	4	5	0.0008	0.0128	0.1342	0.000
9	4	14	0.0008	0.0129	0.1382	0.000
10	5	6	0.0002	0.0026	0.0434	0.000
11	5	8	0.0008	0.0112	0.1476	0.000
12	6	7	0.0006	0.0092	0.1130	0.000
13	6	11	0.0007	0.0082	0.1389	0.000
14	7	8	0.0004	0.0046	0.0780	0.000
15	8	9	0.0023	0.0363	0.3804	0.000
16	9	39	0.0010	0.0250	1.2000	0.000
17	10	11	0.0004	0.0043	0.0729	0.000
18	10	13	0.0004	0.0043	0.0729	0.000
19	13	14	0.0009	0.0101	0.1723	0.000
20	14	15	0.0018	0.0217	0.3660	0.000
21	15	16	0.0009	0.0094	0.1710	0.000
22	16	17	0.0007	0.0089	0.1342	0.000
23	16	19	0.0016	0.0195	0.3040	0.000
24	16	21	0.0008	0.0135	0.2548	0.000

Table A.4: IEEE 39-Bus Test System: Branch Data

Branch Number	From Bus	To Bus	Resistance (pu)	Reactance (pu)	Susceptance (pu)	Branch Tap
25	16	24	0.0003	0.0059	0.0680	0.000
26	17	18	0.0007	0.0082	0.1319	0.000
27	17	27	0.0013	0.0173	0.3216	0.000
28	21	22	0.0008	0.0140	0.2565	0.000
29	22	23	0.0006	0.0096	0.1846	0.000
30	23	24	0.0022	0.0350	0.3610	0.000
31	25	26	0.0032	0.0323	0.5130	0.000
32	26	27	0.0014	0.0147	0.2396	0.000
33	26	28	0.0043	0.0474	0.7802	0.000
34	26	29	0.0057	0.0625	1.0290	0.000
35	28	29	0.0014	0.0151	0.2490	0.000
36	2	30	0.0000	0.0181	0.0000	1.025
37	6	31	0.0000	0.0500	0.0000	1.070
38	6	31	0.0000	0.0500	0.0000	1.070
39	10	32	0.0000	0.0200	0.0000	1.070
40	12	11	0.0016	0.0435	0.0000	1.006
41	12	13	0.0016	0.0435	0.0000	1.006
42	19	20	0.0007	0.0138	0.0000	1.060
43	19	33	0.0007	0.0142	0.0000	1.070
44	20	34	0.0009	0.0180	0.0000	1.009
45	22	35	0.0000	0.0143	0.0000	1.025
46	23	36	0.0005	0.0272	0.0000	1.000
47	25	37	0.0006	0.0232	0.0000	1.025
48	29	38	0.0008	0.0156	0.0000	1.025

A.2 Dynamic Data

Similarly the dynamic data can be classified as:

- Generator Dynamic Data
- Exciter Data
- Governor Data
- PSS Data

Generator Dynamic Data

Table A.5 represents the generator dynamic data. The nomenclature for the table headings is:

X_d	Generator direct-axis synchronous reactance, in per unit
X'_d	Generator quadrature-axis synchronous reactance, in per unit
X_q	Generator direct-axis transient reactance, in per unit
X'_q	Generator quadrature-axis transient reactance, in per unit
R_a	Generator armature resistance, in per unit
T'_d	Direct-axis transient field winding time constant, in sec
T'_q	Quadrature-axis transient field winding time constant, in sec
H	Generator inertia constant, in sec
K_D	Damping coefficient

Table A.5: IEEE 39-Bus Test System: Gen. Dynamic Data

Gen	30	31	32	33	34	35	36	37	38	39
X_d	1.8200	0.9050	0.8650	0.8650	2.0700	0.8650	0.9308	0.9308	1.2356	1.9500
X'_d	0.3420	0.4370	0.2740	0.2740	0.2800	0.2740	0.3503	0.3503	0.2290	0.3400
X_q	1.7910	0.6300	0.5800	0.5800	1.9900	0.5800	0.6706	0.6706	1.2221	1.8700

Table A.5: IEEE 39-Bus Test System: Gen. Dynamic Data

X'_q	0.5500	0.4400	0.2120	0.2120	0.4900	0.2120	0.2652	0.2652	0.3630	0.4275
R_a	0.0015	0.0068	0.0113	0.0113	0.0046	0.0113	0.0024	0.0024	0.0013	0.0020
T'_d	5.30	6.00	7.40	7.40	4.10	7.40	8.00	8.00	4.55	8.00
T'_q	1.500	0.067	0.050	0.050	0.560	0.050	0.040	0.040	0.480	1.500
H	3.5452	3.8554	3.1617	3.1617	2.3186	3.1617	3.0317	3.0317	3.5031	5.3906
K_D	0.0	0.0	0.0	0.0	0.0	0.0	0.0	0.0	0.0	0.0

Exciter Data

Table A.6 represents the exciter data. The nomenclature for the table headings is:

K_A	Amplifier gain, in per unit
T_A	Amplifier time constant, in sec
T_E	Exciter time constant, in sec
K_F	Regulator gain, in per unit
T_F	Regulator time constant, in sec
A_{EX} & B_{EX}	Derived saturation constants for rotating exciters
V_{Rmax}	Regulator maximum output, in per unit
V_{Rmin}	Regulator minimum output, in per unit
E_{fdmax}	Maximum field voltage, in per unit
E_{fdmin}	Minimum field voltage, in per unit

Table A.6: IEEE 39-Bus Test System: Exciter Data

Gen	30	31	32	33	34	35	36	37	38	39
K_A	40	19.5768	15.5969	40	20	40	25	25	30	8.5
T_A	0.03	0.0166	0.0487	0.05	0.03	0.05	0.02	0.02	0.01	0.05

The following exciter parameter values were common for all the generators:

T_E	0.36
K_F	0.12
T_F	0.36
A_{EX}	0.0056
B_{EX}	1.07
V_{Rmax}	8.0
V_{Rmin}	-8.0
E_{fdmax}	8.85
E_{fdmin}	-8.85

Governor Data

Table A.7 represents the governor data. The nomenclature for the table headings is:

R	Turbine droop setting, in %
T_G	Governor time constant, in sec

Table A.7: IEEE 39-Bus Test System: Governor Data

Gen	30	31	32	33	34	35	36	37	38	39
R	3.5452	3.8554	3.1617	3.1617	2.3186	3.1617	3.0317	3.0317	3.5031	5.3906
T_G	1.8200	6.6667	5.0000	5.0000	20.000	5.0000	2.0000	2.0000	10.000	25.000

PSS Data

Table A.8 represents the power system stabilizer data. The nomenclature for the table headings is:

K_{STAB}	Stabilizer gain
T_W	Washout filter time constant, in sec

T_1	Stabilizer lead time constant, in sec
T_2	Stabilizer lag time constant, in sec
V_{Smax}	Stabilizer output upper limit, in per unit
V_{Smin}	Stabilizer output lower limit, in per unit

Table A.8: IEEE 39-Bus Test System: PSS Data

Gen	30	31	32	33	34	35	36	37	38	39
K_{STAB}	1.0	24.4	1.9	1.9	24.4	1.9	15.0	15.0	5.0	24.4
T_W	17.0	3.0	10.0	10.0	3.0	10.0	29.5	29.5	20.0	3.0
T_1	0.350	0.150	0.879	0.879	0.150	0.879	0.280	0.280	0.145	0.150
T_2	0.053	0.050	0.275	0.275	0.050	0.275	0.090	0.090	0.018	0.050
V_{Smax}	0.05	0.05	0.05	0.05	0.05	0.05	0.05	0.05	0.05	0.05
V_{Smin}	-0.05	-0.05	-0.05	-0.05	-0.05	-0.05	-0.05	-0.05	-0.05	-0.05

A.3 Test System Diagram

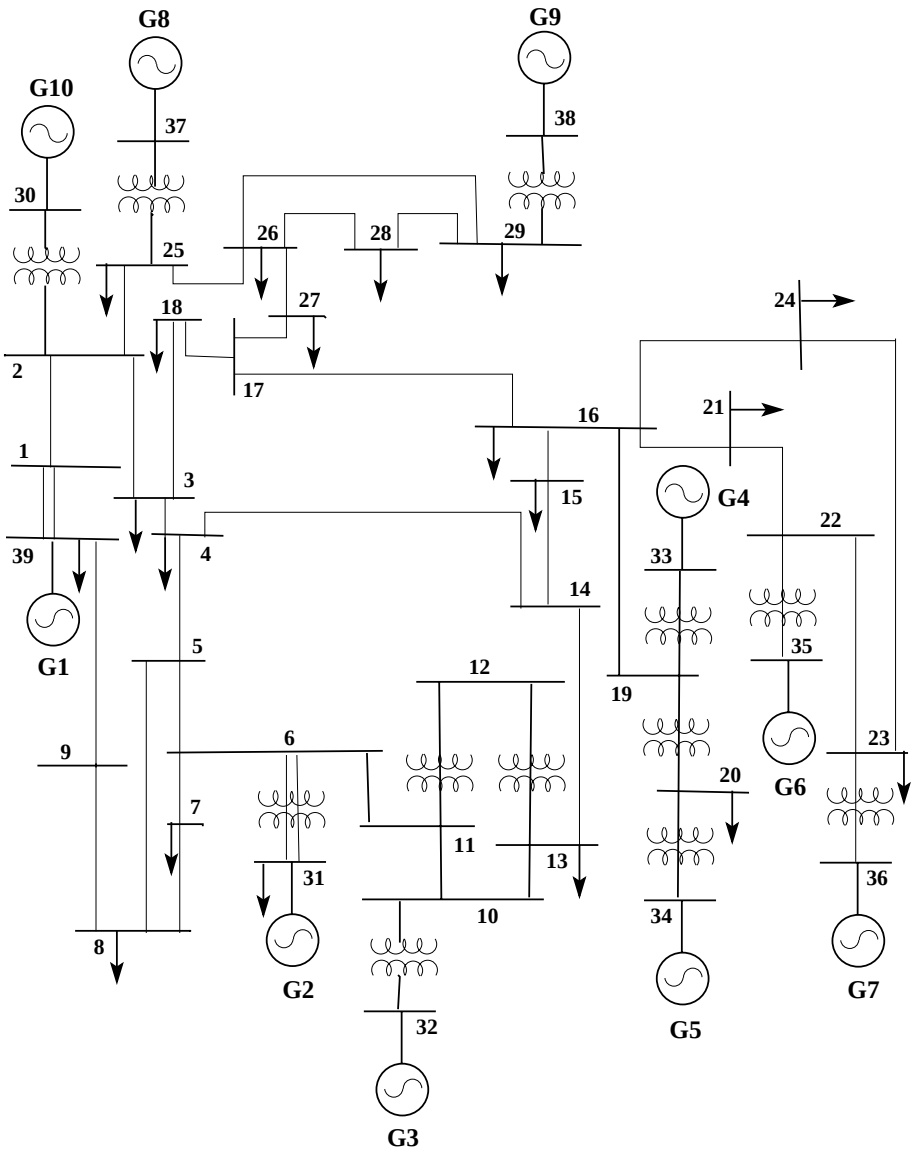

Figure A.1: Single line diagram of the IEEE 39-Bus Test System

A.4 Communication System Topologies

A.4.1 Mesh Topology

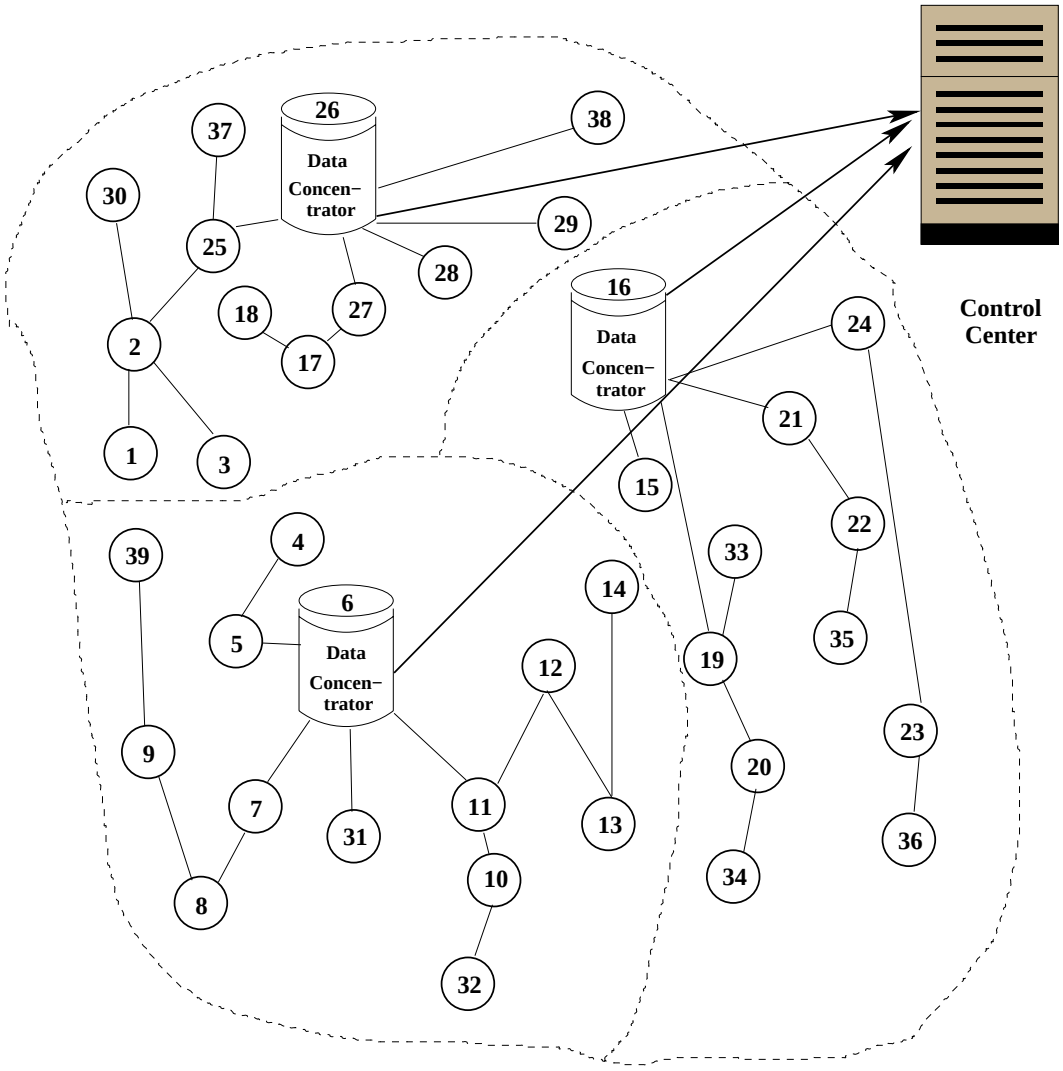

Figure A.2: Schematic diagram of the mesh topology for communications.

A.4.2 Star Topology

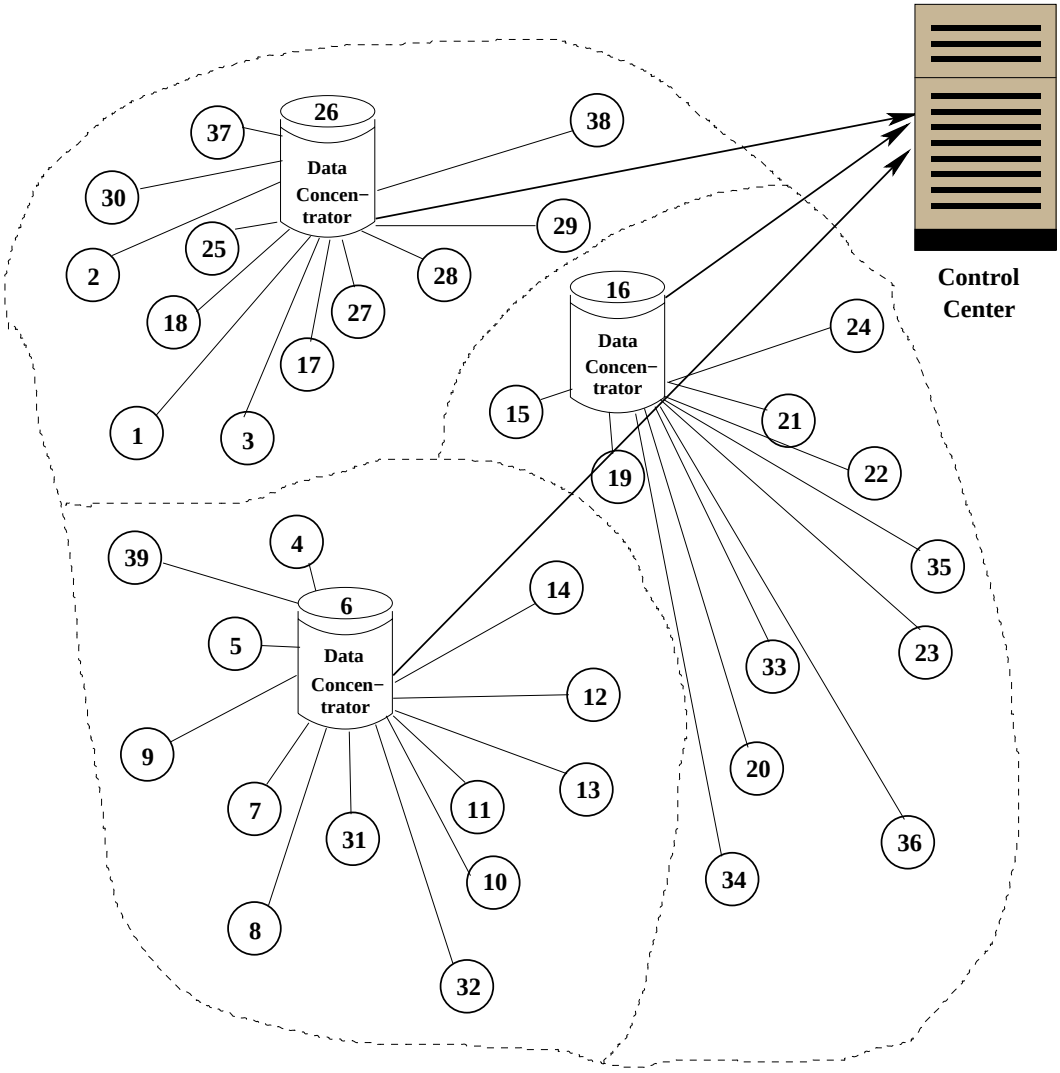

Figure A.3: Schematic diagram of the star topology for communications.

Bibliography

[1] L. Y. Taylor, S. M. Hsu *Transmission Voltage Recovery Following a Fault Event in the Metro Atlanta Area*, IEEE Power Engineering Society Summer Meeting, 2000.

[2] D. N. Kosterev, C. W. Taylor, W. A. Mittelstadt *Model Validation for the August 10, 1996 WSCC System Outage*, IEEE Transactions on Power Systems, Vol. 14, No. 3, August 1999.

[3] L. Vargas, V. H. Quintana, R. Miranda *Voltage Collapse Scenario in the Chilean Interconnected System*, IEEE Transactions on Power Systems, Vol. 14, No. 4, November 1999.

[4] I. A. Hiskens, M. Akke *Analysis of the Nordel Power Grid Disturbance of January 1, 1997 Using Trajectory Sensitivities*, IEEE Transactions on Power Systems, Vol. 14, No. 3, August 1999.

[5] P. Kundur *Power System Stability and Control*, McGraw-Hill Inc. (1993).

[6] Marek Zima *Special Protection Schemes in Electric Power Systems*, Ph. D Literature Survey, Swiss Federal Institute of Technology, Zurich, 2002.

[7] P. M. Anderson, B. K. LeReverend *Industry Experience with Special Protection Schemes*, lEEE Transactions on Power Systems, Vol. 11, No. 3, August 1996.

[8] K. Walve *Modeling Power System Components at Severe Disturbance*, CIGRE Session, Paper No. 38-18, 1986.

[9] Luis G. Perez, Alfred J. Fleschig, Vaithianathan Venkatasubramanian *Modeling the Protective System for Power System Dynamic Analysis*, IEEE Transactions on Power Systems, Vol. 9, No. 4, November 1994.

[10] M. Stubbe, A. Bihain. J. Deuse, J. C. Baader *STAG - A new Unified Software Program for the Study of the Dynamic Behavior of Electric Power Systems*, IEEE Transactions on Power Systems, Vol. 4, No. 1, February 1989.

[11] Peter W. Sauer, M. A. Pai *Power System Dynamics and Stability*, Prentice Hall (1997).

[12] Miroslav Begovic, Borka Mirosevic, Damir Novosel *A Novel Method for Voltage Instability Protection*, Proceedings of the 35^{th} Hawaii International Conference on System Sciences, (2002).

[13] Mauro Paris, Cheryl Johnson, Anjan Bose, David Curtice *Operator Training Simulator: Component Models*, IEEE Transactions on Power Systems, Vol. 4, No. 3, August 1989.

[14] P. M. Anderson *Power System Protection*, McGraw-Hill (1998).

[15] J. Lewis Blackburn *Protective Relaying: Principles and Applications*, 2^{nd} Ed., Marcel Dekker Inc. (1997)

[16] Homer M. Rustebakke(Editor) *Electric Utility Systems and Practices*, 4^{th} Ed., John Wiley and Sons, (1983).

[17] Westinghouse Electric Corporation *Electrical Transmission and Distribution Reference Book*, 4^{th} Ed., East Pittsburgh, (1964).

[18] Electric Power Research Institute *Transmission Line Reference Book:* $345kV$ *and Above*, 2^{nd} Ed., EPRI, Palo Alto, California, (1982).

[19] C. W. Taylor, D. C. Erickson, K. E. Martin, V. Venkatasubramanian, R. E. Wilson *WACS–Wide Area Stability and Voltage Control System: R & D and On-Line Demonstration*, submitted to IEEE Proceedings special issue on Energy Infrastructure Defense Systems.

[20] C. Y. Chung, L. Wang, F. Howell, P. Kundur *Generation Rescheduling Methods to Improve Power Transfer Capability Constrained by Small-Signal Stability*, IEEE Transactions on Power Systems, Vol. 19, No. 1, February 2004.

[21] G. T. Heydt *Computer Analysis Methods for Power Systems*, Macmillan Publishing Company (1986).

[22] B. Stott *Power Systems Dynamic Response Calculations*, Proc. IEEE, Vol. 67, February 1979.

[23] P. M. Anderson, A. A. Fouad *Power System Control and Stability*, 2^{nd} Ed., Wiley-IEEE Press (2002).

[24] Arthur R. Bergen, Vijay Vittal *Power System Analysis*, 2^{nd} Ed., Prentice Hall (2000).